

The Kinase Inhibitor Sorafenib Induces Cell Death through a Process Involving Induction of Endoplasmic Reticulum Stress^{∇†}

Mohamed Rahmani, Eric Maynard Davis, Timothy Ryan Crabtree, Joseph Reza Habibi, Tri K. Nguyen, Paul Dent, and Steven Grant*

Departments of Medicine, Biochemistry, and Pharmacology, Virginia Commonwealth University, School of Medicine, Richmond, Virginia 23298

Received 15 June 2006/Returned for modification 29 September 2006/Accepted 17 May 2007

Sorafenib is a multikinase inhibitor that induces apoptosis in human leukemia and other malignant cells. Recently, we demonstrated that sorafenib diminishes Mcl-1 protein expression by inhibiting translation through a MEK1/2-ERK1/2 signaling-independent mechanism and that this phenomenon plays a key functional role in sorafenib-mediated lethality. Here, we report that inducible expression of constitutively active MEK1 fails to protect cells from sorafenib-mediated lethality, indicating that sorafenib-induced cell death is unrelated to MEK1/2-ERK1/2 pathway inactivation. Notably, treatment with sorafenib induced endoplasmic reticulum (ER) stress in human leukemia cells (U937) manifested by immediate cytosolic-calcium mobilization, GADD153 and GADD34 protein induction, PKR-like ER kinase (PERK) and eukaryotic initiation factor 2 α (eIF2 α) phosphorylation, XBP1 splicing, and a general reduction in protein synthesis as assessed by [³⁵S]methionine incorporation. These events were accompanied by pronounced generation of reactive oxygen species through a mechanism dependent upon cytosolic-calcium mobilization and a significant decline in GRP78/Bip protein levels. Interestingly, enforced expression of IRE1 α markedly reduced sorafenib-mediated apoptosis, whereas knockdown of IRE1 α or XBP1, disruption of PERK activity, or inhibition of eIF2 α phosphorylation enhanced sorafenib-mediated lethality. Finally, downregulation of caspase-2 or caspase-4 by small interfering RNA significantly diminished apoptosis induced by sorafenib. Together, these findings demonstrate that ER stress represents a central component of a MEK1/2-ERK1/2-independent cell death program triggered by sorafenib.

The discovery that aberrant activation of the Ras-Raf-MEK1/2-ERK1/2 module occurs in a high percentage (30%) of human cancers (12, 42, 48, 57) provided a rationale for attempting to disrupt this pathway as a candidate anticancer strategy. Recently, a number of specific inhibitors designed to interrupt this pathway at the level of Ras, Raf, or MEK1/2 have been developed. Among these, sorafenib, a biaryl urea, also known as BAY 43-9006 or Nexavar, was initially developed as a specific inhibitor of C-Raf and B-Raf. However, subsequent studies revealed that it also inhibits several other tyrosine kinases involved in tumor progression, including VEGFR-2, VEGFR-3, PDGFR- β , Flt3, c-Kit, and Ret (6, 60). Interestingly, sorafenib has been shown to inhibit mutant (^{V600E})B-Raf kinase activities in vitro and to diminish MEK/extracellular signal-regulated kinase (ERK) activation in various tumor cell lines, including those harboring mutant Ras or B-Raf (25, 56, 60). Although this compound has potent activity in preclinical tumor xenograft models against a variety of tumor cell types (60), has shown promising activity in a number of clinical trials, and has recently been approved for the treatment of advanced renal cell carcinoma (51), the mechanism(s) by which it exerts

its antitumor activity has not been fully elucidated and is currently the subject of ongoing investigation (40).

In recent communications, we and other investigators reported that sorafenib induced marked mitochondrial damage manifested by cytochrome *c* and apoptosis-inducing factor release into the cytosol, caspase activation, and apoptosis in various tumor cells, including human leukemia cells (40, 45, 67). Furthermore, sorafenib was found to downregulate myeloid cell leukemia 1 (Mcl-1) protein expression through inhibition of translation in a MEK1/2-ERK1/2 signaling-independent mechanism (45). Moreover, Mcl-1 downregulation was shown to play an important functional role in sorafenib-mediated lethality (45, 67). These findings bring into question the notion that sorafenib exerts its lethal effects by a straightforward, linear inhibition of the Raf-1–MEK1/2–ERK1/2 module. Mcl-1 is a multidomain antiapoptotic member of the Bcl-2 family (7) and was originally identified in myeloid leukemia cells undergoing maturation (28). Subsequently, it was shown that Mcl-1 plays a central role in the survival of malignant human hematopoietic cells (i.e., myeloma and leukemia) (13, 35). However, results of several studies indicate that Mcl-1 downregulation by itself is insufficient to trigger apoptosis (37), suggesting that other mechanisms may be involved in the rapid and extensive apoptosis induced by agents such as sorafenib in human leukemia cells (45).

Currently, very little is known about the mechanism(s) by which sorafenib triggers cell death. In this communication, we provide evidence that sorafenib mediates cell death in human leukemia cells through a MEK1/2-ERK1/2 signaling-independent mechanism. Significantly, we demonstrate for the first

* Corresponding author. Mailing address: Division of Hematology/Oncology, MCV Station Box 230, Virginia Commonwealth University, Richmond, VA 23298. Phone: (804) 828-5211. Fax: (804) 828-8079. E-mail: stgrant@hsc.vcu.edu.

† Supplemental material for this article may be found at <http://mc.manuscriptcentral.com/mcb>.

[∇] Published ahead of print on 4 June 2007.

time that sorafenib potently induces endoplasmic reticulum (ER) stress manifested by a rapid mobilization of cytoplasmic calcium, activation of PKR-like ER kinase (PERK), induction of IRE1 α and XBP1 splicing, phosphorylation of eukaryotic translation initiation factor 2 α (eIF2 α), inhibition of protein translation, and induction of GADD153 and GADD34. In addition, these events are associated with the calcium-dependent production of reactive oxygen species (ROS). Collectively, these findings provide a novel framework for understanding the mechanism of action of sorafenib and possibly for the rational integration of this agent into antileukemic regimens.

MATERIALS AND METHODS

Plasmids and cell transfection. The human leukemia U937, Jurkat, and K562 cells were cultured as previously reported (47). Wild-type murine embryonic fibroblast (MEF) cells and MEF cells in which eIF2 α was genetically replaced by a nonphosphorylatable form of eIF2 α (eIF2 α Ser 51/A) in both alleles were obtained from C. Koumenis (University of Pennsylvania). A Myc-tagged PERK Δ C construct (3) was a generous gift from J. A. Diehl (University of Pennsylvania Cancer Center, Philadelphia, PA), and hemagglutinin (HA)-tagged human wild-type IRE1 α (22) was kindly provided by C. Hetz and L. H. Glimcher (Harvard Medical School). Human dominant-negative eIF2 α (eIF2 α -DN) cDNA was PCR amplified from pCMV-eIF2 α -S51A (27) and cloned into pcDNA3.1/V5-His (Invitrogen) in frame with V5 peptide. Each of these constructs was individually transfected into K562 cells by using an Amaxa nucleofector (Koeln, Germany) as previously described (10). Stable single PERK Δ C, HA-IRE1 α , or V5-eIF2 α -DN cell clones were selected in the presence of 1 μ g/ml of puromycin, 400 μ g/ml of hygromycin, or 400 μ g/ml of geneticin, respectively. Thereafter, cells derived from each clone were analyzed for Myc tag, HA tag, or V5 tag expression, respectively, by Western blot analysis. A Tet-On Jurkat cell line inducibly expressing constitutively active MEK1 or constitutively active C-Raf under doxycycline control was previously described (47, 68). Leukemic blasts were isolated from peripheral blood samples obtained with informed consent from several patients with acute myeloblastic leukemia (AML), FAB subtype M2, as previously described (45).

Knockdown experiments involving transient transfection with siRNA and stable transfection with short hairpin RNA (shRNA) or short hairpin microRNA (shRNAmir). Cells were transfected with a negative-control small interfering RNA (siRNA) directed against firefly luciferase (Dharmacon, Lafayette, CO) or siRNA directed against PERK, GCN2, GADD153, caspase-2, or XBP1 (Dharmacon) using an Amaxa nucleofector. Cells were left in culture for 24 to 48 h prior to exposure to different treatment regimens.

U937 cells stably expressing shRNA directed against IRE1 α , caspase-3, caspase-4, caspase-9, TRAF2, or JNK1/2 were generated as follows. Two cDNA oligonucleotides containing the targeted sequence were synthesized, annealed, and cloned into the pSUPER.retro.neo vector (Oligoengine, Seattle, WA) by using standard techniques. The sequences used were IRE1 α (5'-GAGAAGATGATTGCGATGGAT-3'), caspase-3 (5'-AGGTGGCAACAGAATTGAGT-3'), caspase-4 (5'-AATGTACTGAACTGGAAGGAA-3'), caspase-9 (5'-ACAGATGCCTGGTTGCTTTAA-3'), TRAF2 (the same target sequence as that previously reported [59], 5'-CGACATGAACATCGCAAGC-3'), and JNK1/2 (the same target sequence as that previously reported [30], 5'-TGAAAGAATGTCCTACCTT-3'). An shRNA directed against green fluorescent protein (GFP) (GGTATGTACAGGAACGCA) obtained from Ambion (Austin, TX) was cloned into the pSUPER.retro.neo plasmid as described above and served as a control for various shRNA-expressing cells. The constructs were verified by DNA sequencing and transfected into U937 cells by using an Amaxa nucleofector. Stable clones were selected in the presence of 400 μ g/ml geneticin and screened by Western blot analysis for reduced expression levels compared to those of control U937 cells transfected with GFP shRNA.

K562 cells in which heme-regulated inhibitor (HRI) was knocked down were obtained by stable transfection with the lentiviral vector pLKO.1, coding for HRI-specific shRNA (Open Biosystems, Huntsville, AL). The sequence used was 5'-GAATTGGTAGAAGGTGTGTTT-3'. A construct coding for enhanced GFP (eGFP)-shRNA was used as a control. Stable clones were selected in the presence of puromycin as indicated above.

To knock down PKR in K562 cells, we used an shRNAmir strategy. Briefly, K562 cells were transfected with the pSM2c shRNAmir construct targeting human PKR

(Open Biosystems), and single clones were selected in the presence of 1 μ g/ml puromycin and screened for reduced expression of PKR protein as described above. The sequence used to target PKR was 5'-TGCTGTTGACAGTGAGCGCGCAGGGAGTAGTACTTAAATATAGTGAAGCCACAGATGTATATTTAAGTACTACTCCCTGCTTGCCTACTGCCTCGGA-3'. K562 cells transfected with the eGFP-shRNAmir construct were used as a control for PKR shRNAmir cells.

Reagents. Sorafenib was provided by Bayer Pharmaceuticals Corporation (West Haven, CT) and the National Cancer Institute, NIH (Bethesda, MD). It was dissolved in dimethyl sulfoxide, and aliquots were maintained at -80°C . MnTBAP and BAPTA-AM were purchased from Calbiochem (San Diego, CA), and thapsigargin, tunicamycin, and polyethylene glycol (PEG)-catalase were purchased from Sigma (St. Louis, MO). PD184352 was described previously (11), and U0126 was purchased from Cell Signaling Technology (Beverly, MA). All reagents were prepared and used as recommended by their suppliers.

Assessment of apoptosis. The extent of cell death was routinely assessed by annexin V-fluorescein isothiocyanate-propidium iodide staining as previously described (44). 7-Amino-actinomycin D staining was also used with MEF cells as previously described (44).

Immunoblotting. Immunoblotting was performed using whole-cell lysates as previously described in detail (44). The primary antibodies used in this study were caspase-4 (Stressgene Bioreagents, Ann Arbor, MI); ATF6 (Imgenex, San Diego); caspase-2, phospho-ERK1/2 (Thr202/Tyr204), phospho-MEK1/2, phospho-eIF2 α , phospho-PERK, and IRE1 α (Cell Signaling Technology); GADD153, eIF2 α , GRP78, GRP94, GADD34, XBP1, HRI, PKR, ERK1/2, and Myc tag (Santa Cruz Biotechnology, Santa Cruz, CA); GCN2 (Bethyl Laboratories, Montgomery, TX); and α -tubulin (Calbiochem).

Protein synthesis. Sorafenib-treated U937 cells were pulse-labeled with 100 μ Ci/ml of [^{35}S]methionine-[^{35}S]cysteine (ICN, Biomedicals, Inc., Irvine, CA) for 1 h, washed in phosphate-buffered saline (PBS), and lysed in lysis buffer as described above. Equal amounts of proteins were separated on sodium dodecyl sulfate-polyacrylamide gel electrophoresis gel and electrotransferred to nitrocellulose membranes. The membranes were then subjected to autoradiography to visualize the newly synthesized proteins and subsequently stained with ponceau S solution (Sigma) to detect the total amounts of proteins on the membranes.

RT-PCR and XBP1 splicing. Total RNA was extracted from treated or untreated cells by using an RNeasy kit (QIAGEN) and then subjected to reverse transcription (RT)-PCR by using an AccuScriptTM high-fidelity first-strand cDNA synthesis kit (Stratagene). The cDNAs were PCR amplified using specific primers for XBP1, PERK, and 18S. The primers used were XBP1 forward (5'-GAG TTA AGA CAG CGC TTG GG-3'), XBP1 reverse (5'-GGTAAGG AACTGGTCTT-3'), PERK forward (5'-CTCACAGGCAAGGAAGGA G-3'), and PERK reverse (5'-AACAACTCAAAGCCACCAC-3'). The primers for the ribosomal 18S RNA, which served as an internal standard, were obtained from SuperArray Bioscience Corporation (Bethesda, MD).

Determination of ROS. ROS production was monitored as described previously (46). Briefly, following treatment, cells were incubated with 1 μ g/ml CM-H2DCFDA (Molecular Probes, Eugene, OR) for 30 min, after which they were washed with PBS, and the amount of fluorescence was determined using a Becton-Dickinson FACScan flow cytometer.

Intracellular-Ca $^{2+}$ measurements. Intracellular-calcium levels were measured using Fluo3-AM. Briefly, cells were washed twice in Ca $^{2+}$ -free PBS, loaded with 5 μ M Fluo3-AM for 30 min, and washed twice in Ca $^{2+}$ -free PBS. Cells were then resuspended in RPMI 1640 medium with 10% fetal bovine serum and subjected to treatment with drugs for the indicated times, after which cells were washed in Ca $^{2+}$ -free PBS. Finally, cells were resuspended in Ca $^{2+}$ -free PBS and the fluorescence intensities which reflect changes in cytosol-free Ca $^{2+}$ concentration were measured using a Becton-Dickinson FACScan flow cytometer.

Statistical analysis. The significance of the differences between the experimental conditions was determined using Student's *t* test for unpaired observations.

RESULTS

Sorafenib-mediated lethality is independent of MEK/ERK pathway inactivation. We previously reported that exposure to sorafenib resulted in a time- and dose-dependent inactivation of ERK1/2 in several human leukemia cell types (45). Western blot analysis revealed that sorafenib-mediated ERK1/2 dephosphorylation correlated closely with MEK1/2 dephosphorylation (Fig. 1A). To investigate the role of MEK1/2-ERK1/2 inactivation in sorafenib-induced apoptosis, we employed Jur-

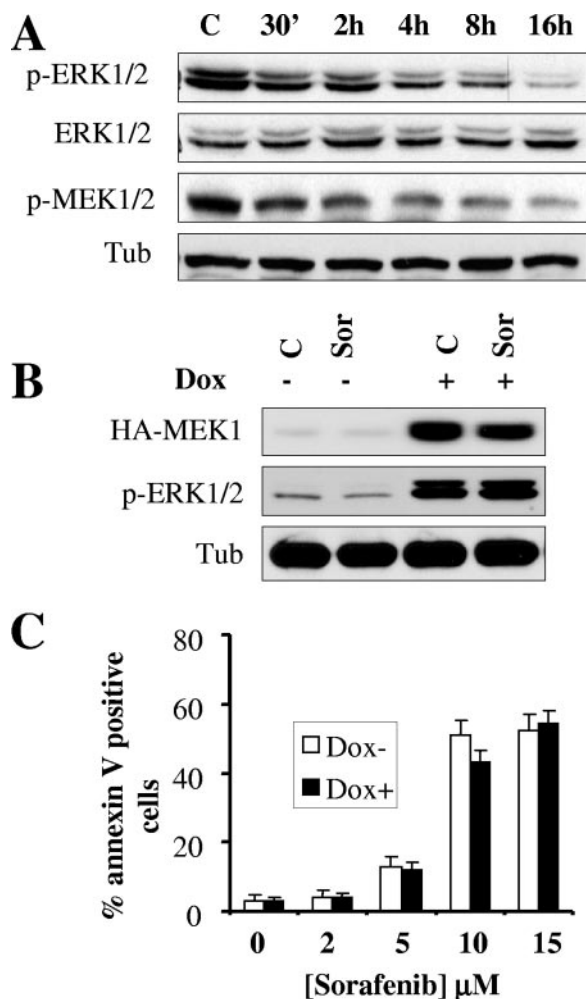


FIG. 1. Inducible activation of the MEK/ERK pathway does not prevent sorafenib-mediated cell death. (A) U937 cells were exposed to 10 μM sorafenib for the designated intervals, after which cell lysates were obtained and subjected to Western blot analysis to monitor expression of ERK1/2, phospho-ERK1/2, and phospho-MEK1/2. For this and all subsequent Western blot analyses, blots were subsequently reprobed with antitubulin (Tub) antibodies to document equivalent loading and transfer. The results of a representative study are shown; two additional experiments yielded equivalent results. (B) Jurkat cells (MT6) inducibly expressing constitutively active HA-tagged MEK1 were left untreated or treated for 24 h with 2 $\mu\text{g}/\text{ml}$ doxycycline (Dox). Cells were then exposed to 10 μM sorafenib (Sor) for an additional 4 h, after which protein lysates were prepared and analyzed for HA-MEK1 and phospho-ERK1/2 expression. Alternatively, cells were treated for 24 h, after which the extent of apoptosis was determined using an annexin V staining assay (C). Values represent the means \pm standard deviations for at least three separate experiments performed in triplicate. C, control.

kat cells (MT6) inducibly expressing a constitutively active MEK1 protein under the control of a doxycycline-responsive promoter. As shown in Fig. 1B, addition of doxycycline resulted in the pronounced induction of constitutively active MEK1 protein levels and phospho-ERK1/2 in both control and sorafenib-treated cells. However, exposure to sorafenib resulted in equivalent inductions of cell death in the absence and the presence of doxycycline (Fig. 1C). Similar results were obtained with two additional MEK1-inducible clones and with

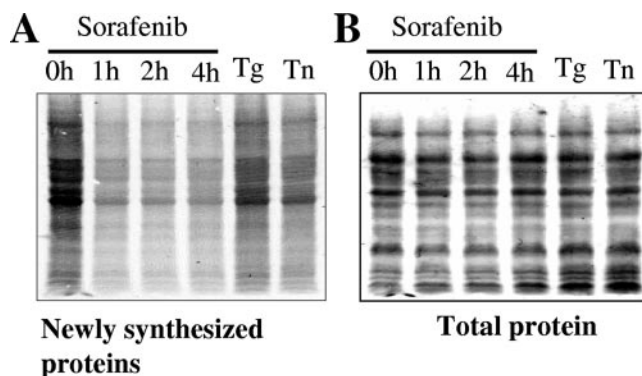


FIG. 2. Exposure to sorafenib results in global translation inhibition. U937 cells were exposed to 10 μM sorafenib for the designated intervals and 0.5 μM thapsigargin or 0.5 $\mu\text{g}/\text{ml}$ tunicamycin for 4 h and then pulsed with [^{35}S]methionine for an additional 1 h. The cells were subsequently lysed, and protein lysates were separated on sodium dodecyl sulfate-polyacrylamide gel electrophoresis gel and transferred to a nitrocellulose membrane. The amounts of newly synthesized proteins were detected by autoradiography (A), and subsequently, the total amounts of proteins on the membranes were visualized by staining with ponceau S solution (B). The results shown are representative of three separate experiments.

U937 cells stably expressing constitutively active MEK1 (46) (data not shown). These findings are consistent with results obtained with Jurkat cells inducibly expressing a constitutively active Raf1 construct under the control of a doxycycline-responsive promoter as shown in Fig. S1 in the supplemental material. While addition of doxycycline induced a robust increase in C-Raf expression as well as ERK1/2 phosphorylation, sorafenib (10 μM) clearly inhibited ERK1/2 phosphorylation in the absence or presence of doxycycline (see Fig. S1A in the supplemental material), indicating that sorafenib targets wild-type as well as constitutively active C-Raf. It should be noted that levels of phosphorylated ERK1/2 in sorafenib-treated cells were nevertheless higher in the presence of doxycycline than in its absence (see Fig. S1A in the supplemental material). Importantly, enforced expression of constitutively active C-Raf and the resulting ERK1/2 activation in cells exposed to doxycycline did not significantly protect them from sorafenib-mediated lethality ($P > 0.05$) (see Fig. S1B in the supplemental material). These observations are consistent with the previous findings indicating that enforced activation of MEK1 is unable to confer resistance to sorafenib in human leukemia cells. Together, these findings argue that inactivation of the MEK1/2-ERK1/2 module does not play a central role in sorafenib-mediated lethality and imply that other, perhaps unrelated, actions are involved.

Treatment with sorafenib inhibits protein synthesis in a dose-dependent manner. Recently, we reported that sorafenib inhibits Mcl-1 protein synthesis and that this phenomenon contributes at least in part to the lethal action of this agent (45). Therefore, we questioned whether treatment with sorafenib inhibited translation of other proteins or whether instead this phenomenon was restricted to Mcl-1. To this end, time course studies of newly synthesized proteins were performed. As shown in Fig. 2A, exposure of U937 cells to 10 μM sorafenib for 1, 2, and 4 h resulted in a marked decrease in [^{35}S]methionine incorporation. Treatment of cells for 4 h with

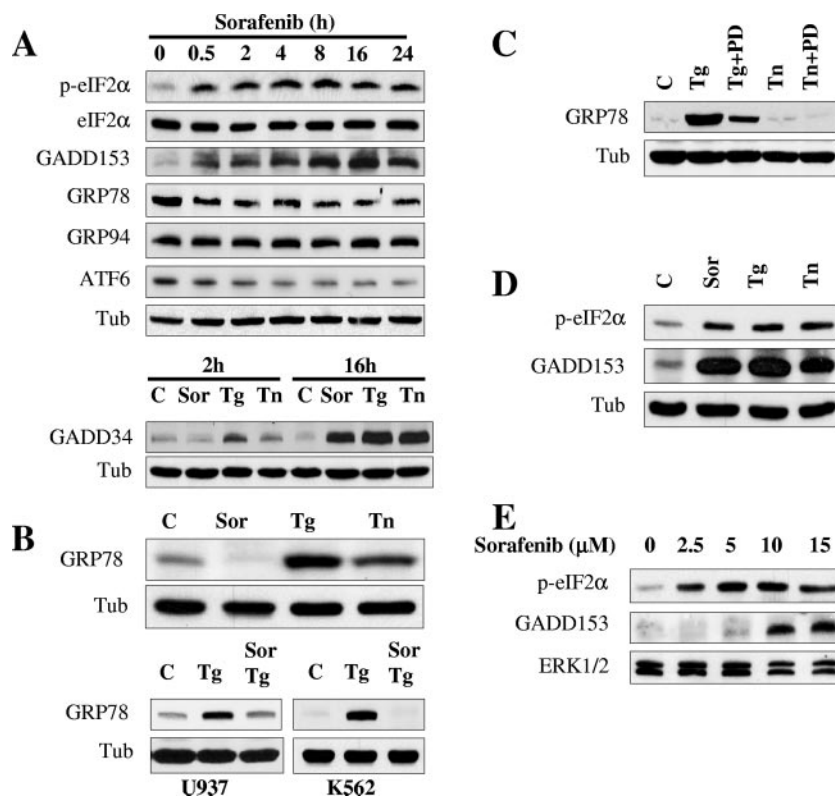


FIG. 3. Sorafenib triggers the UPR in human leukemia cells. (A, upper) U937 cells were exposed to 10 μ M sorafenib for the designated intervals, after which protein lysates were prepared and subjected to Western blot analysis using the indicated antibodies. (A, lower) U937 cells were exposed to 10 μ M sorafenib (Sor), 0.5 μ M thapsigargin (Tg), or 0.5 μ g/ml tunicamycin (Tn) for 2 or 16 h, after which Western blot analysis was performed as described above. (B, upper) U937 cells were exposed to 10 μ M sorafenib, 0.5 μ M thapsigargin, or 0.5 μ g/ml tunicamycin for 16 h, after which protein lysates were prepared and subjected to Western blot analysis to monitor GRP78 expression. (B, lower) U937 and K562 cells were exposed to sorafenib (10 μ M) and thapsigargin (0.5 and 1 μ M, respectively) alone or together for 6 h, after which protein lysates were prepared and subjected to Western blot analysis. (C) K562 cells were treated with 1 μ M thapsigargin or 1 μ g/ml tunicamycin in the presence or absence of 10 μ M PD184352 for 16 h, after which protein lysates were prepared and subjected to Western blot analysis to monitor GRP78 expression. (D) K562 cells were exposed to 10 μ M sorafenib for 4 h, after which cells were lysed and Western blot analysis was performed to monitor eIF2 α phosphorylation and GADD153 expression. (E) Leukemia blasts were isolated from the peripheral blood of a patient with AML (FAB classification M2) and exposed to the designated concentration of sorafenib for 6 h, after which cells were lysed and protein was subjected to Western blot analysis to monitor eIF2 α phosphorylation and GADD153 expression. For each experiment, at least two additional studies yielded equivalent results. C, control; Tub, antitubulin antibody.

thapsigargin (0.5 μ M) or tunicamycin (0.5 μ g/ml), two agents known to inhibit protein synthesis, also resulted in a decrease in protein synthesis, although these agents were less effective than sorafenib, at least at these concentrations. In contrast, total protein levels visualized by ponceau S staining were similar (Fig. 2B). These findings indicate that sorafenib does not selectively down-regulate Mcl-1 expression but instead exerts a more global inhibitory effect on protein synthesis in leukemia cells.

Sorafenib induces the UPR independently of MEK1/2-ERK1/2 pathway inactivation. Protein synthesis in eukaryotic cells is primarily controlled at the level of translation initiation (43, 52). Furthermore, inhibition of protein synthesis represents one of the cardinal features of the unfolded protein response (UPR), a compensatory cellular defense mechanism which is activated by stresses stemming from the burden of misfolded proteins (61, 63). Therefore, the possibility that sorafenib might elicit the UPR was investigated. In view of the well-established role of eIF2 α in protein translation initiation and in view of evidence that this factor undergoes phosphory-

lation and inhibits protein synthesis in response to a variety of apoptotic stimuli (17, 21, 62), the possibility that this factor might be affected by exposure of leukemic cells to sorafenib was examined first. As shown in Fig. 3A, exposure to sorafenib (10 μ M) resulted in the rapid phosphorylation of eIF2 α as early as 30 min after drug exposure, an event that was sustained over the ensuing 24 h. In contrast, no major changes were detected in eIF2 α total protein levels. Further analysis revealed that treatment with sorafenib for 4 h resulted in a dose-dependent phosphorylation of eIF2 α similar to those observed with thapsigargin (0.5 μ M) and tunicamycin (0.5 μ g/ μ l) (data not shown), two agents whose abilities to induce ER stress and eIF2 α phosphorylation are well documented (17, 21). GADD153 protein, a member of the CAAT/enhancer binding protein (C/EBP) family known to accumulate after eIF2 α phosphorylation (19, 55), displayed a clear increase in expression 30 min after treatment with sorafenib, an event which also persisted through the entire treatment interval (24 h) (Fig. 3A). In addition, the protein levels of the phosphatase PP1 activator GADD34, which is believed to facilitate eIF2 α

dephosphorylation and ultimately mediate translational recovery (26, 39), underwent marked increases after 16 h of exposure, comparable to responses observed in cells exposed to thapsigargin or tunicamycin (Fig. 3A, lower). There was also a significant decline in expression of ATF6 (90 kDa) in sorafenib-treated cells, which was first apparent 2 to 4 h following drug exposure.

Interestingly, the glucose-regulated protein GRP78/Bip, a chaperone protein classically induced during the UPR (54), underwent a rapid decline (i.e., by 30 min) in sorafenib-treated cells, an event which persisted over the entire treatment interval (24 h) (Fig. 3A). On the other hand, no major change was observed in protein levels of GRP94, another chaperone protein. However, consistent with the results of numerous studies, the ER stress inducers thapsigargin and tunicamycin increased the expression of GRP78 in U937 (Fig. 3B, upper) as well as in Jurkat (data not shown) cells. Furthermore, sorafenib abrogated thapsigargin-mediated GRP78 expression in both U937 and K562 cells (Fig. 3B, lower). In view of evidence that GRP78 plays a cytoprotective role in the setting of ER stress (34), these findings raise the possibility that blockade of GRP78 induction may contribute to sorafenib-mediated lethality. Further analysis suggested that MEK1/2 activation was required for thapsigargin-mediated induction of GRP78 in K562 cells, as the MEK1/2 inhibitor PD184352 (11) essentially abrogated this phenomenon (Fig. 3C). Interestingly, with these cells, treatment for 16 h with tunicamycin (1 $\mu\text{g}/\text{ml}$), unlike thapsigargin treatment, did not induce GRP78 (Fig. 3C). In contrast to these actions, sorafenib mimicked the actions of thapsigargin and tunicamycin in inducing eIF2 α phosphorylation and GADD153 accumulation in Bcr-abl⁺ K562 leukemia cells (Fig. 3D), in Jurkat lymphoid leukemia cells (data not shown), and in primary human leukemia (AML) blasts (Fig. 3E). Together, these findings demonstrate that sorafenib induces rapid phosphorylation of the translation initiation factor eIF2 α and accumulation of GADD153 and GADD34 proteins, classical markers of the UPR, raising the possibility that ER stress may be involved in the apoptotic response of human leukemia cells to sorafenib. They also suggest that the failure of sorafenib to induce GRP78, in contrast to the result for thapsigargin, may stem from inhibition of the Raf/MEK1/2 cascade.

To test the possibility that sorafenib-mediated eIF2 α phosphorylation might be related to MEK/ERK inactivation, we employed Jurkat cells (MT6) inducibly expressing a constitutively active MEK1 construct under the control of a doxycycline-responsive promoter. As shown in Fig. 4A, addition of doxycycline resulted in a substantial increase in expression of constitutively active MEK1 and phospho-ERK1/2 in both control and sorafenib-treated cells. However, exposure to sorafenib induced equivalent increases in eIF2 α phosphorylation and GADD153 accumulation in the absence and the presence of doxycycline. Furthermore, Western blot analysis revealed that the MEK1/2 inhibitor U0126 was unable to increase eIF2 α phosphorylation or GADD153 accumulation. Notably, the effects of sorafenib were similar to those of thapsigargin and tunicamycin rather than MEK1/2 inhibitors in this regard (Fig. 4B). Collectively, these findings argue strongly that sorafenib increases eIF2 α phosphorylation and GADD153 accumulation

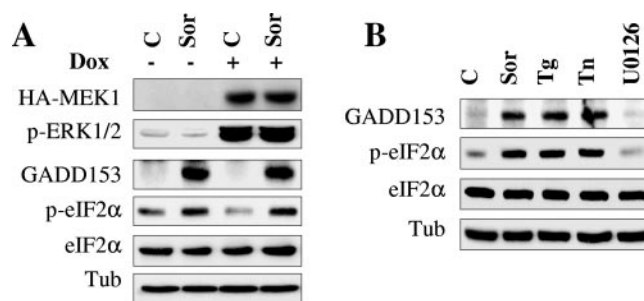


FIG. 4. Sorafenib triggers the UPR independently of MEK/ERK inactivation. (A) Jurkat cells (MT6) inducibly expressing constitutively active HA-tagged MEK1 were left untreated or treated for 24 h with 2 $\mu\text{g}/\text{ml}$ doxycycline (Dox) and then exposed to 10 μM sorafenib (Sor) for an additional 4 h. Cells were then lysed, and Western blot analysis was performed using the designated antibodies. (B) U937 cells were treated with 10 μM sorafenib, 0.5 μM thapsigargin (Tg), 0.5 $\mu\text{g}/\text{ml}$ tunicamycin (Tn), and 10 μM U0126 for 4 h, after which protein lysates were prepared and subjected to Western blot analysis using the indicated antibodies. For each experiment, at least two additional studies yielded equivalent results. C, control; Tub, antitubulin antibody.

through a mechanism unrelated to interruption of the MEK1/2-ERK1/2 axis.

Lastly, attempts were made to determine whether GADD153 accumulation might play a functional role in sorafenib-mediated cell death. To this end, Jurkat leukemia cells were transiently transfected with siRNA directed against GADD153. Western blot analysis revealed that GADD153 induction by sorafenib was essentially abrogated in GADD153 siRNA-transfected cells (see Fig. S2A in the supplemental material). However, no major effect on apoptosis was observed ($P > 0.05$ for cells transfected with GADD153 siRNA versus cells transfected with NC siRNA) (see Fig. S2B in the supplemental material). These findings argue against the possibility that GADD153 induction plays a major role in sorafenib-mediated apoptosis.

Inhibition of PERK activity by siRNA or dominant-negative PERK reduces eIF2 α phosphorylation and enhances sorafenib-mediated cell death. To date, four kinases are known to phosphorylate eIF2 α : PKR, GCN2, PERK, and HRI. Of these, PERK has been most commonly implicated in the ER stress response (19, 21, 27). Western blot analysis revealed that sorafenib induced a pronounced increase in PERK phosphorylation, an effect that was considerably more pronounced than those of thapsigargin and tunicamycin, potent inducers of ER stress (Fig. 5A). Phosphorylation of PERK by sorafenib was also observed in K562 cells (data not shown). To determine whether PERK plays a functional role in eIF2 α phosphorylation induced by sorafenib, two strategies were employed. First, K562 leukemia cells were transiently transfected with siRNA directed against PERK, resulting in a significant decrease in PERK mRNA level but no reduction in the internal standard 18S RNA (Fig. 5A). Significantly, phosphorylation of eIF2 α in cells transfected with PERK siRNA was substantially reduced compared to that in cells transfected with negative-control siRNA following treatment with sorafenib for 2 or 4 h ($P < 0.05$) (Fig. 5A). In parallel, apoptosis was monitored after 24 h of exposure of cells to sorafenib (10 μM) in the presence or absence of PERK siRNA. As shown in Fig. 5B, apoptosis was

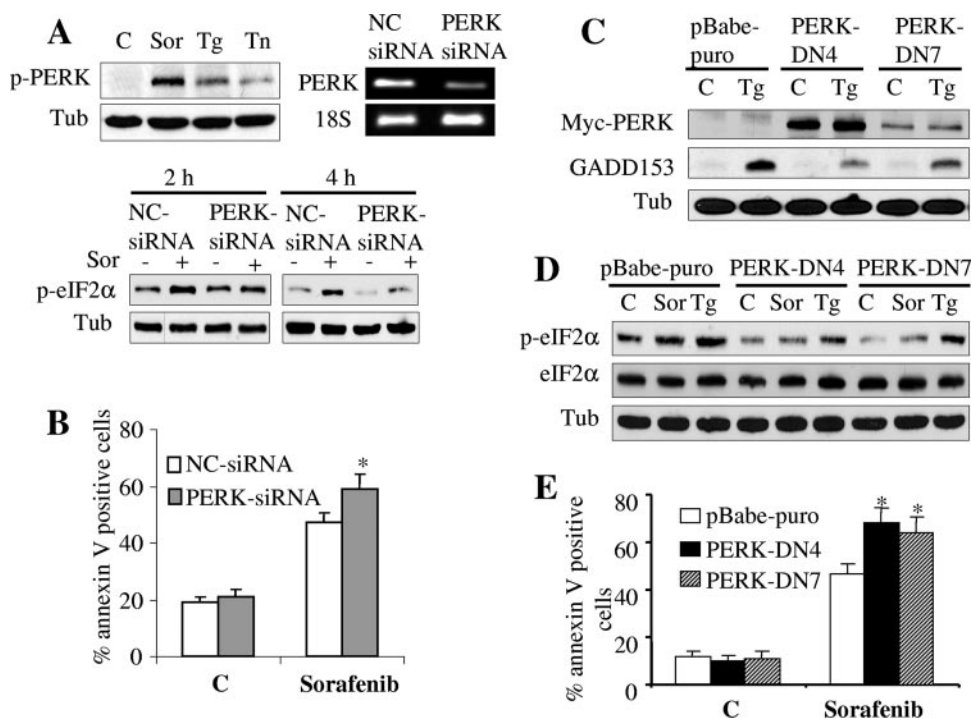


FIG. 5. Inhibition of PERK activity reduces eIF2 α phosphorylation and enhances sorafenib-mediated cell death. (A, upper left) U937 cells were exposed to 10 μ M sorafenib (Sor), 0.5 μ M thapsigargin (Tg), or 0.5 μ g/ml tunicamycin (Tn) for 16 h, after which protein lysates were prepared and subjected to Western blot analysis to monitor PERK phosphorylation. (A, upper right) K562 cells were transiently transfected with siRNA against PERK or with negative-control (NC) siRNA and incubated for 48 h, after which PERK mRNA levels were quantified by RT-PCR. Alternatively, transfected cells were treated with 10 μ M sorafenib for 2 or 4 h, after which protein lysates were prepared and subjected to Western blot analysis to monitor eIF2 α phosphorylation (A, lower). Alternatively, cells were treated for 24 h, after which the extent of cell death was monitored using annexin V staining (B). (C) Two clones (PERK-DN4 and PERK-DN7) of K562 cells stably expressing dominant-negative PERK and empty-vector cells (pBabe-puro) were treated with 1 μ M thapsigargin for 2 h, after which protein lysates were prepared and subjected to Western blot analysis to monitor myc-tagged PERK and GADD153 protein expression. (D) Dominant-negative PERK clones and empty-vector K562 cells were treated with 10 μ M sorafenib or 1 μ M thapsigargin for 2 h, after which cell lysates were prepared and subjected to Western blot analysis. Alternatively, annexin V analysis was performed after 24 h of treatment to monitor the extent of cell death (E). For all annexin V studies, values represent the means \pm standard deviations for at least three separate experiments performed in triplicate. *, significantly higher than values obtained for empty-vector pBabe-puro cells ($P < 0.05$). C, control; Tub, antitubulin antibody.

modestly but significantly increased ($P < 0.05$) in PERK siRNA-transfected cells. Next, K562 cells were stably transfected with a PERK Δ C construct which functions as a PERK dominant-negative construct (3). Two separate clones, designated PERK-DN4 and PERK-DN7, were examined. As previously reported (19), dominant-negative PERK markedly inhibited GADD153 accumulation in cells exposed to thapsigargin (Fig. 5C). Consistent with results obtained with PERK siRNA, dominant-negative PERK partially attenuated eIF2 α phosphorylation mediated by sorafenib as well as that mediated by thapsigargin (Fig. 5D). In accord with results obtained with PERK siRNA, cells transfected with dominant-negative PERK were also significantly more sensitive to sorafenib-mediated lethality than controls ($P < 0.05$ in each case) (Fig. 5E). Together, these findings implicate PERK in the eIF2 α phosphorylation response to sorafenib and suggest that in this setting PERK may play a protective role against sorafenib-mediated lethality.

Sorafenib mediates eIF2 α phosphorylation independently of HRI, PKR, or GCN2, and this event opposes the lethal actions of sorafenib. To determine whether eIF2 α phosphorylation plays a functional role in sorafenib-mediated lethality, K562 cells were stably transfected with an eIF2 α construct

(V5-tagged eIF2 α -DN) in which serine 51 was mutated to alanine and consequently acted as a dominant-negative construct of eIF2 α . Western blot analysis revealed that cells ectopically expressing eIF2 α -DN exhibited a significant attenuation of sorafenib- or thapsigargin-mediated eIF2 α phosphorylation (Fig. 6A). Notably, these cells were modestly but significantly more sensitive to sorafenib-mediated apoptosis (Fig. 6B). In addition, MEF cells in which the endogenous eIF2 α has been genetically replaced by a nonphosphorylatable form of eIF2 α (eIF2 α Ser 51/A) in both alleles were also markedly more sensitive to sorafenib-mediated lethality than control MEF cells expressing wild-type eIF2 α (Fig. 6C). These findings suggest that eIF2 α phosphorylation plays a protective role against sorafenib-mediated apoptosis.

To determine whether the other eIF2 α kinases, HRI, PKR, and GCN2, contribute to eIF2 α phosphorylation in response to sorafenib, a stable knockdown experiment using shRNA against HRI (HRI-shRNA), microRNA directed against PKR (PKR-RNAmir), and transient transfection with siRNA against GCN2 was performed. Western blot analysis revealed that HRI and PKR proteins were significantly knocked down in HRI-shRNA- and PKR-RNAmir-transfected K562 cells, re-

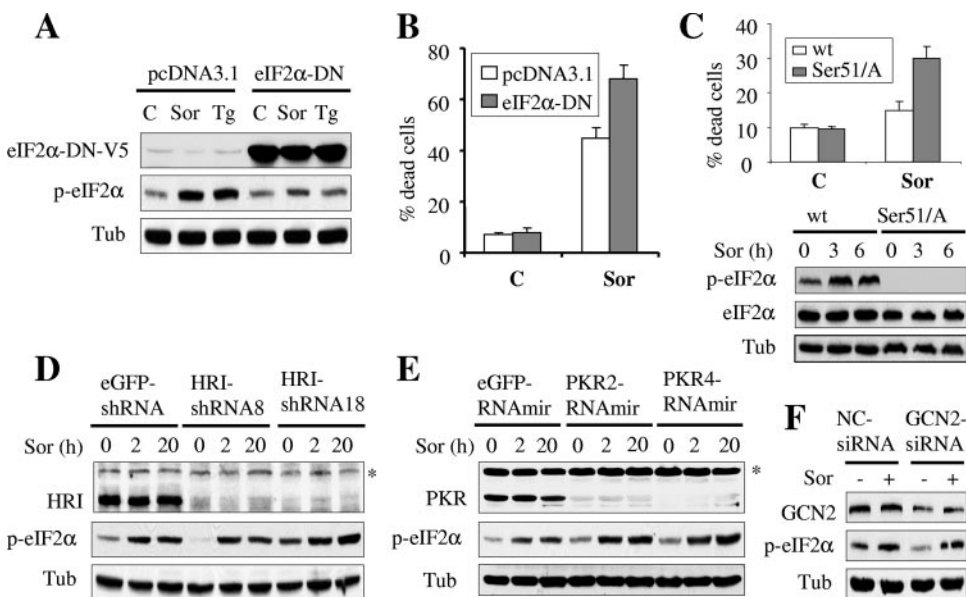


FIG. 6. Sorafenib fully induces eIF2α phosphorylation in HRI, PKR, or GCN2 knockdown cells, an event that opposes sorafenib-mediated lethality. (A) K562 cells expressing V5-tagged eIF2α-DN (cl-9) or their controls (pcDNA3.1) were treated with sorafenib (Sor) or thapsigargin (Tg) for 2 h, after which protein lysates were prepared and subjected to Western blot analysis. Alternatively, the extent of apoptosis was determined using an annexin V staining assay after 24 h of exposure to sorafenib (B). Values represent the means for three separate experiments ± standard deviations. (C) Wild-type MEF (wt) in which eIF2α was intact and MEF cells in which endogenous eIF2α was genetically replaced by a nonphosphorylatable form of eIF2α (eIF2α ser 51/A) in both alleles were treated with 12 μM sorafenib for 24 h, after which the extent of cell death was determined using a 7-amino-actinomycin D assay (upper). Alternatively, cells were lysed at 3 and 6 h posttreatment and the protein lysates were subjected to Western blot analysis (lower). (D) Two clones (HRI-shRNA8 and HRI-shRNA18) of K562 cells stably transfected with an shRNA construct against HRI and cells transfected with an shRNA construct directed against eGFP were exposed to sorafenib for 2 h and 20 h, after which protein lysates were prepared and subjected to Western blot analysis to monitor HRI protein levels and eIF2α phosphorylation. (E) Two K562 clones (PKR2-RNAmir and PKR4-RNAmir) in which PKR was knocked down using shRNAmir and their control counterparts (eGFP-shRNAmir) were treated with sorafenib for 2 h and 20 h; then, PKR levels and eIF2α phosphorylation were monitored using Western blot analysis. An asterisk indicates nonspecific bands for HRI and PKR blots. (F) K562 cells were transiently transfected with siRNA against GCN2 or negative-control (NC) siRNA for 48 h. Cells were then exposed to 10 μM sorafenib for an additional 2 h, after which cells were lysed and protein lysates were subjected to Western blot analysis to monitor expression of GCN2 and eIF2α. C, control; Tub, antitubulin antibody.

spectively (Fig. 6D and E, respectively). However, sorafenib-induced eIF2α phosphorylation in these cells was comparable to that in control cells after 2 h and 20 h of sorafenib exposure (Fig. 6D and E). Similarly, reductions in GCN2 protein levels induced by siRNA did not prevent sorafenib-mediated eIF2α phosphorylation (Fig. 6F). In separate studies, time course analysis of cells exposed to sorafenib revealed no major changes in the expression and phosphorylation of these kinases (data not shown). Consistent with these findings, knockdown of these kinases did not confer significant resistance to sorafenib (see Fig. S3 in the supplemental material). Together, these findings argue against a major role for HRI, PKR, and GCN2 in triggering eIF2α phosphorylation or lethality in cells exposed to sorafenib. Taken in conjunction with the previous observations, these findings instead support the notion that sorafenib mediates eIF2α phosphorylation primarily through activation of PERK.

Sorafenib induces a marked increase in IRE1α protein level and promotes XBP1 splicing, events that antagonize the lethal action of sorafenib. In addition to PERK, activating transcription factor 6 (ATF6) and inositol-requiring enzyme 1 (IRE1) represent two other ER transmembrane proteins that serve as ER stress sensors and mediate the UPR. Activation of IRE1 promotes X-box binding protein 1 (XBP1) mRNA splicing, an event that is required for translation of activated/spliced XBP1

(XBP1s), a potent transcription factor (5, 65). Attempts were therefore undertaken to determine whether sorafenib might activate IRE1/XBP1. As shown in Fig. 7A, exposure of U937 cells to 10 μM sorafenib resulted in a marked accumulation of IRE1α protein, an event that was analogous to that which occurred with thapsigargin or tunicamycin treatment. This was associated with a modest but readily apparent induction of the spliced form of XBP1 (XBP1s, 50 kDa) (Fig. 7B). Consistent with these observations, XBP1 mRNA splicing was also observed in U937 cells (Fig. 7B), although this effect was less pronounced than that obtained following exposure to tunicamycin (0.5 μg/ml). Higher concentrations of sorafenib (e.g., 15 or 20 μM) resulted in more pronounced splicing in XBP1 mRNA (data not shown). In contrast, neither sorafenib (10 μM) nor tunicamycin (1 μg/ml) induced XBP1 splicing in K562 cells when administered at these concentrations (Fig. 7B).

To determine the functional significance of these findings, multiple strategies were employed. First, IRE1α was stably knocked down in U937 cells by using shRNA against IRE1α (Fig. 7C, inset). Notably, these cells were considerably more sensitive to sorafenib (7.5 μM) than control GFP-transfected cells (Fig. 7C). Conversely, K562 cells were stably transfected with an HA-tagged IRE1α construct, and two clones (IRE-cl7 and IRE-cl13) displaying increased IRE1α protein levels were employed (Fig. 7D, left). Notably, cells overexpressing IRE1α

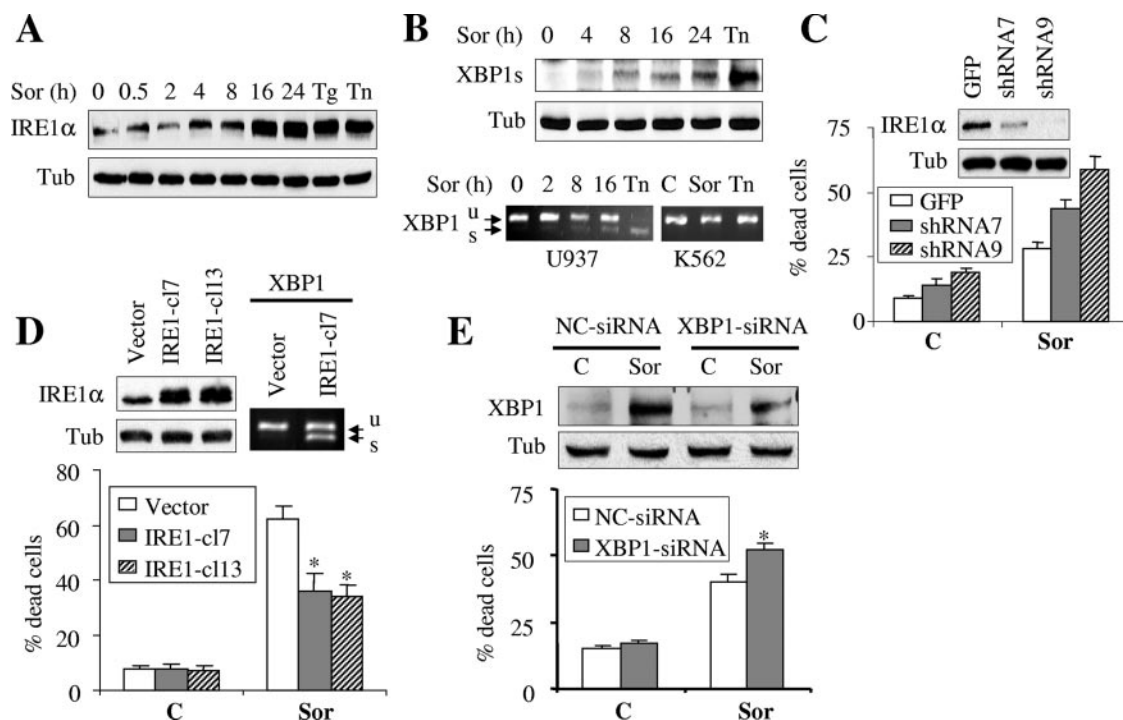


FIG. 7. Functional role of IRE1/XBP1 splicing and TRAF2/JNK1 in cell response to sorafenib. (A and B) U937 cells were exposed to sorafenib (Sor; 10 μ M) for the designated intervals or thapsigargin (Tg; 0.5 μ M) or tunicamycin (Tn; 0.5 μ g/ml) for 16 h, after which cell lysates were obtained and subjected to Western blot analysis to monitor IRE1 α (A) and spliced XBP1 (XBP1s; 50 kDa) (B, upper) protein levels. (B, lower) U937 and K562 cells were exposed to sorafenib (10 μ M) for the designated intervals or tunicamycin (0.5 μ g/ml for U937 and 1 μ g/ml for K562 cells) for 16 h, after which XBP1 splicing (XBP1s, spliced; XBP1u, unspliced) was monitored using RT-PCR as described in Materials and Methods. (C) Two clones (shRNA7 and shRNA9) of U937 cells in which IRE1 α was knocked down using shRNA and GFP-shRNA-transfected cells were treated with 7.5 μ M sorafenib for 24 h, after which the extent of apoptosis was determined using an annexin V staining assay. (C, inset) Western blot analysis performed on lysates prepared from cells prior to treatment. (D, upper left) Western blot analysis performed on lysates prepared from two K562 cell clones (IRE1-cl7 and IRE1-cl13) expressing human HA-tagged IRE1 α and their control counterparts (K562 cells transfected with pMSCVhyg empty vector). (D, upper right) XBP1 mRNA splicing was monitored by RT-PCR in IRE1-cl7 and their control empty-vector cells. (D, lower) IRE1-cl7, IRE1-cl13, and empty-vector cells were treated with 10 μ M sorafenib for 28 h, after which the extent of apoptosis was determined using an annexin V staining assay. Values represent the means for three separate experiments \pm standard deviations. *, significantly lower than values for empty-vector-transfected cells ($P < 0.01$). (E) U937 cells were transiently transfected with siRNA directed against XBP1 or negative-control (NC) siRNA for 24 h. Cells were then exposed to 7.5 μ M sorafenib for an additional 24 h, after which cells were lysed and protein lysates were subjected to Western blot analysis to monitor expression of spliced XBP1. Alternatively, the extent of apoptosis was determined by monitoring annexin V staining. Values represent the means for three separate experiments \pm standard deviations. *, significantly higher than values for NC transfected cells ($P < 0.05$). C, control; Tub, antitubulin antibody.

were significantly more resistant to sorafenib than the empty-vector-transfected cells (Fig. 7D, lower). Consistent with results from a previous report employing HeLa cells (65), ectopic expression of IRE1 α (IRE-cl7) resulted in XBP1 mRNA splicing (Fig. 7D). Similar results were obtained with IRE-cl13 cells (data not shown). Finally, transient experiments using siRNA against XBP1 revealed that knockdown of XBP1 modestly albeit significantly enhanced sorafenib-mediated lethality in U937 cells (Fig. 7E). Together, these findings suggest that activation of IRE1 α /XBP1 plays an important protective role against sorafenib-mediated lethality.

Previous studies have demonstrated that in cells experiencing ER stress, cross talk occurs between IRE1 α , TRAF2, and apoptosis signal-regulated kinase 1 (ASK1), events that lead to Jun N-terminal protein kinase (JNK) activation and apoptosis (38). In addition, we have previously reported that sorafenib induced JNK activation in human leukemia cells (45). Therefore, the hypothesis that TRAF2-ASK1-JNK might play a role in the apoptotic action of sorafenib was examined. To this end, U937 cells were

stably transfected with constructs coding for shRNA directed against TRAF2 or JNK1/2. As shown in Fig. S4A and S4B in the supplemental material, two clones exhibiting significant knockdown of TRAF2 and JNK1/2 proteins were employed. While cells in which TRAF2 protein levels were substantially reduced exhibited marked sensitivity to tumor necrosis factor alpha (5 ng/ml)-mediated cell death, they were equally sensitive to sorafenib compared to control GFP-shRNA cells ($P > 0.05$) (see Fig. S4A in the supplemental material). Consistent with these observations as well as previous findings indicating that the pharmacologic JNK inhibitor SP600125 did not prevent Mcl-1 downregulation (45) or lethality (M. Rahmani et al., unpublished data), knocking down JNK1/2 did not exert a significant effect on the sensitivities of U937 cells to the lethal action of sorafenib ($P > 0.05$) (see Fig. S4B in the supplemental material). These findings argue against a major role for the TRAF2-ASK1-JNK1/2 axis in sorafenib-mediated cell death.

Exposure to sorafenib induces caspase-2 and caspase-4 processing. Several recent studies have implicated caspase-2 and

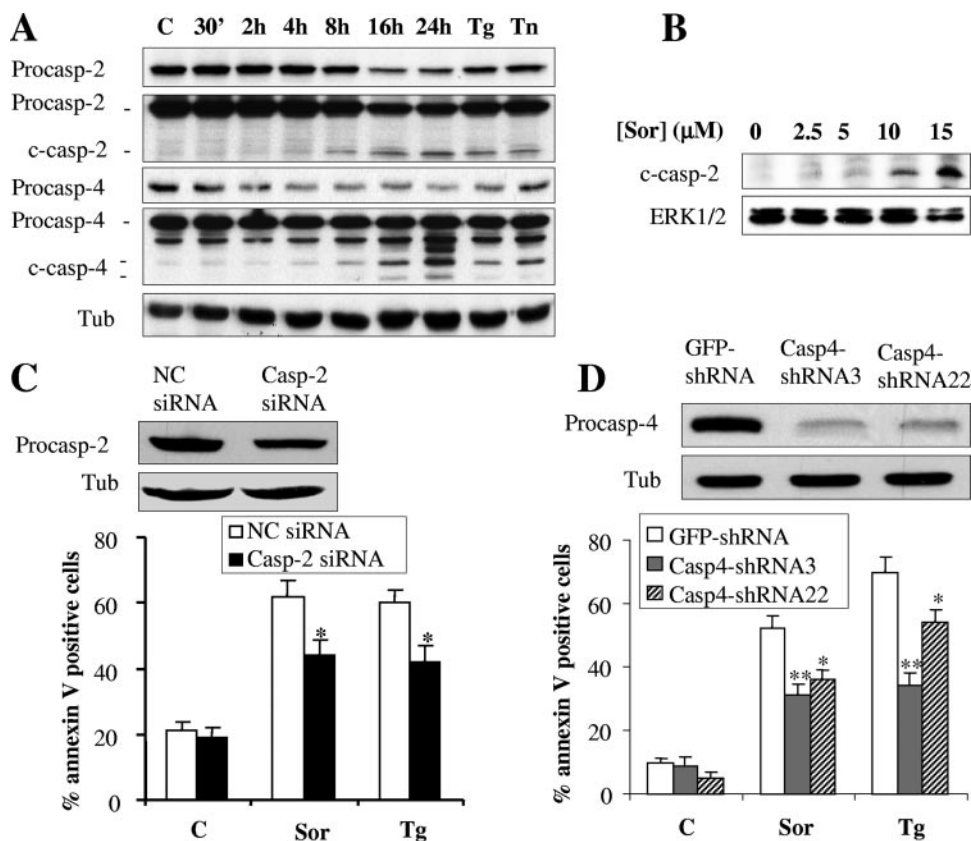


FIG. 8. Treatment with sorafenib results in caspase-2 and caspase-4 processing. (A) U937 cells were exposed to 10 μ M sorafenib (Sor) for the designated intervals or to 0.5 μ M thapsigargin (Tg) or 0.5 μ g/ml tunicamycin (Tn) for 16 h, after which protein lysates were prepared and subjected to Western blot analysis to monitor the protein levels of procaspase-2 (procasp-2) and procaspase-4 (procasp-2) and their cleavage products (c-casp-2 and c-casp-4, respectively). Note that high as well as low exposures of the blots were utilized to facilitate visualization of the decline in expression of the procaspases and the appearance of their cleavage fragments. (B) Leukemia blasts were isolated from the peripheral blood of a patient with AML (FAB classification M2) and exposed to the designated concentration of sorafenib (Sor) for 6 h, after which cells were lysed and protein was subjected to Western blot analysis to monitor caspase-2 processing. The blot was reprobbed with ERK1/2 antibodies to document equivalent loading and transfer. (C) Jurkat cells were transiently transfected with siRNA directed against caspase-2 or negative-control (NC) siRNA for 24 h. Cells were then exposed to 10 μ M sorafenib or 1 μ M thapsigargin (Tg) for an additional 24 h, after which cells were lysed and protein lysates were subjected to Western blot analysis to monitor expression of caspase-2. Alternatively, the extent of apoptosis was determined using an annexin V staining assay. Values represent the means for three separate experiments \pm standard deviations. *, significantly lower than values for NC transfected cells ($P < 0.02$). (D) Two U937 clones (casp4-shRNA3 and casp4-shRNA22) in which caspase-4 was knocked down and their control counterparts (GFP-shRNA) were monitored for expression of procaspase-4 by using Western blot analysis (upper). Alternatively, cells were exposed to 10 μ M sorafenib (Sor) or 0.5 μ M thapsigargin (Tg) for 24 h, after which the extent of cell death was monitored using an annexin V staining assay (lower). Values represent the means for three separate experiments \pm standard deviations. * and **, significantly lower than values for GFP-shRNA cells ($P < 0.02$ and $P < 0.01$, respectively). C, control; Tub, antitubulin antibody.

caspase-4 activation in ER stress induction-mediated cell death (8, 9, 23). The issue of whether these caspases might be activated in response to sorafenib was therefore investigated. As shown in Fig. 8A, both caspase-2 and caspase-4 were processed in cells exposed to sorafenib for 8 to 16 h, analogous to responses of cells to thapsigargin or tunicamycin, a potent inducer of ER stress. Similarly, dose-dependent cleavage of caspase-2 was observed in primary AML blasts after 6 h of treatment with sorafenib (Fig. 8B). To determine whether caspase-2 and caspase-4 play a functional role in sorafenib-mediated cell death, stable- and transient-transfection approaches were employed. To this end, Jurkat leukemia cells were transiently transfected with siRNA directed against caspase-2. Western blot analysis revealed that protein levels of caspase-2 were substantially decreased in cells transfected with caspase-2 siRNA compared to levels obtained with con-

trol siRNA (Fig. 8C). For caspase-4, U937 cells were stably transfected with a construct encoding an shRNA directed against caspase-4. As shown in Fig. 8D, two clones of U937 cells expressing marked decreases in caspase-4 levels were employed. Notably, the extent of cell death induced by sorafenib was significantly reduced in cells in which caspase-2 or caspase-4 was knocked down, analogous to results obtained with thapsigargin (Fig. 8C or D, respectively). Together, these findings suggest that caspase-2 and caspase-4 activation, an event recently linked to the ER stress response (8, 9, 23), contributes functionally to sorafenib-mediated cell death. They also provide further support for the notion that sorafenib induces cell death through an ER stress-dependent mechanism.

In our previous report, we showed that sorafenib induced a marked cleavage of caspase-9 and caspase-3 in human leukemia cells (45). To determine whether caspase-9 and caspase-3

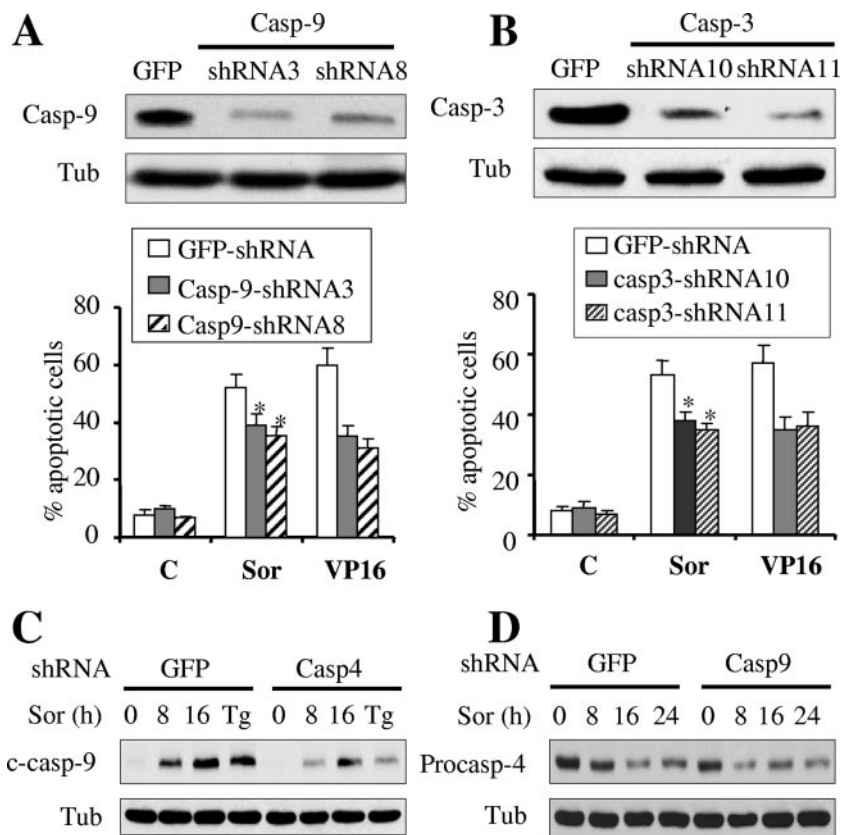


FIG. 9. Caspase-3 or caspase-9 knockdown modestly but significantly protects cells from sorafenib-mediated lethality. (A) Protein lysates were prepared from two clones of U937 cells transfected with caspase-9 shRNA (casp9-shRNA3 and casp9-shRNA8) and from GFP-shRNA-transfected cells and subjected to Western blot analysis (upper). Alternatively, these cells were treated with 10 μ M sorafenib (Sor) or 2.5 μ M VP16 for 24 h, after which the extent of apoptosis was determined using an annexin V staining assay (lower). (B) Protein lysates were prepared from two clones of U937 cells transfected with caspase-3 shRNA (casp3-shRNA10 and casp3-shRNA11) and from GFP-shRNA-transfected cells and subjected to Western blot analysis (upper). Alternatively, these cells were exposed to sorafenib (10 μ M) and VP16 (2.5 μ M) for 24 h and then subjected to an annexin V staining assay (lower). (C and D) Casp4-shRNA3 (C), casp9-shRNA8 (D), and GFP-shRNA cells were treated with sorafenib (10 μ M) for the designated intervals or with thapsigargin (Tg; 0.5 μ M) for 16 h, after which protein lysates were prepared and subjected to Western blot analysis. *, significantly less than values for controls ($P < 0.05$). C, control; Tub, antitubulin antibody.

contribute to sorafenib-mediated cell death, caspase-9 or caspase-3 was stably knocked down in U937 cells by using cells transfected with shRNA directed against these caspases, as shown in Fig. 9A or B, respectively. Notably, knockdown of caspase-3 or caspase-9, which resulted in marked resistance to VP-16-mediated apoptosis, only modestly attenuated, albeit significantly, sorafenib-mediated lethality (Fig. 9A and B) ($P < 0.05$ for caspase-3 or caspase-9 knockdown versus control cells). In addition, the cleavage product of caspase-9 in caspase-4 shRNA cells was substantially reduced compared to that in control cells after treatment with sorafenib, similar to results obtained with thapsigargin (Fig. 9C). In contrast, knocking down caspase-9 had no effect on sorafenib-mediated caspase-4 processing (Fig. 9D). These findings suggest that caspase-9 activation lies downstream of caspase-4, supporting a model in which the apical caspase activated by sorafenib is caspase-4, leading in turn, at least in part, to caspase-9 and caspase-3 activation and apoptosis.

Exposure to sorafenib results in cytosolic-calcium mobilization independently of MEK1/2-ERK1/2 pathway inactivation. Depletion of luminal ER calcium stores is believed to reflect

ER stress which, under certain circumstances, can promote induction of the UPR (58, 66, 69). The question of whether exposure to sorafenib resulted in intracellular-calcium modulation was therefore examined. As shown in Fig. 10A, treatment with sorafenib resulted in a rapid increase in cytosolic-calcium levels (i.e., by 15 min) in U937 as well as in Jurkat cells. Similar results were obtained with K562 cells (data not shown). Furthermore, sorafenib had no effect on calcium mobilization in U937 cells in which ER calcium stores were depleted by pretreatment with thapsigargin for 90 min (Fig. 10B), suggesting that the ER represents a source of calcium release following exposure of cells to sorafenib. To determine whether the protective effect of IRE1 α or PERK against sorafenib-mediated lethality involves attenuation of perturbations in calcium homeostasis, calcium mobilization was investigated in cells expressing dominant-negative PERK or overexpressing IRE1 α (see Fig. S5 in the supplemental material). Notably, sorafenib-mediated cytosolic-calcium mobilization was not significantly increased in dominant-negative PERK cells, nor was it attenuated in IRE1 α -overexpressing cells, suggesting that the cytoprotective actions of IRE1 α and PERK proceed through a

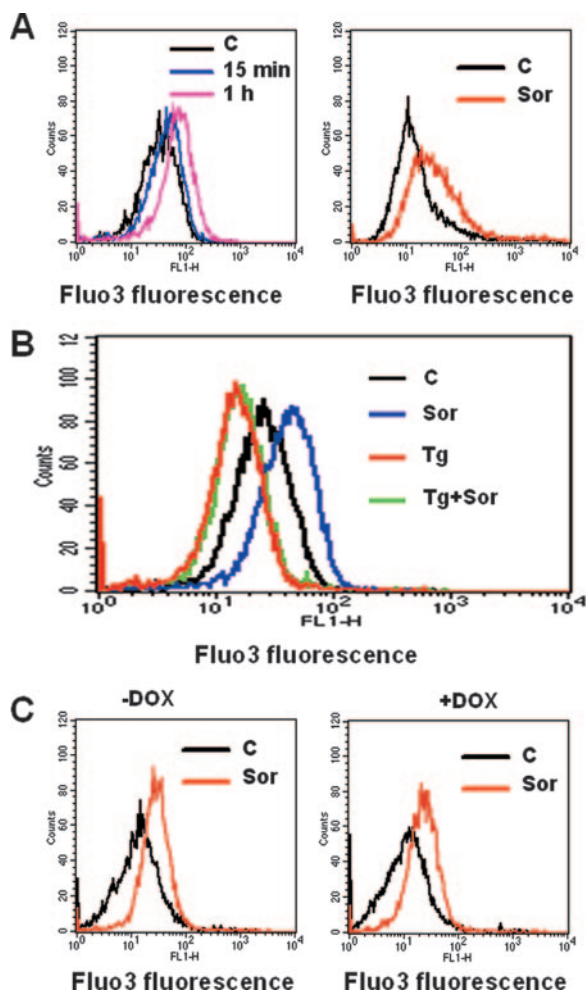


FIG. 10. Treatment with sorafenib results in a potent calcium mobilization in leukemia cells. (A) U937 (left) and Jurkat (right) cells were loaded with Fluo3-AM for 30 min, after which cells were exposed to 10 μ M sorafenib (Sor) for the designated intervals (U937) or 1 h (Jurkat), after which cytosolic calcium was monitored by flow cytometry as indicated in Materials and Methods. (B) U937 cells were loaded with Fluo3-AM for 30 min and then pretreated with thapsigargin (Tg) for 90 min, after which cells were exposed to 10 μ M sorafenib for 1 h; then, the intensity of the fluorescence was monitored by flow cytometry. (C) Jurkat cells inducibly expressing constitutively active MEK1 were left untreated (left) or treated with 2 μ g/ml doxycycline (DOX) (right) for 24 h and then loaded with Fluo3-AM for 30 min and exposed to 10 μ M sorafenib (Sor) for an additional 1 h. The intensity of the fluorescence was then monitored by flow cytometry. For each experiment, the results of a representative study are shown; at least two additional experiments yielded equivalent results. C, control.

mechanism independent of calcium mobilization. Lastly, activation of the MEK1/2-ERK1/2 pathway by doxycycline in Jurkat cells inducibly expressing constitutively active MEK1 did not prevent an increase in cytoplasmic calcium (Fig. 10C), demonstrating that this event is not related to MEK1/2-ERK1/2 inactivation.

Sorafenib induces the rapid and robust generation of ROS through a calcium-dependent but MEK1/2-ERK1/2 signaling-independent mechanism. Several lines of evidence indicate that increased cytosolic-Ca²⁺ concentrations can promote increases in ROS production originating primarily in the mito-

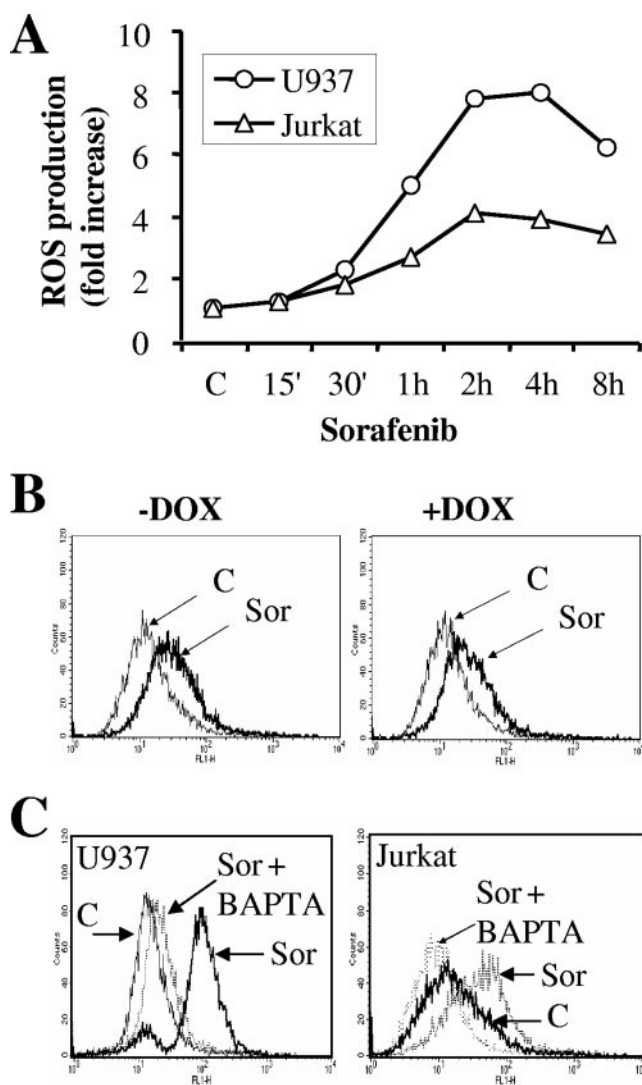


FIG. 11. Exposure to sorafenib results in a dramatic increase in calcium-dependent ROS production. (A) U937 and Jurkat cells were exposed to 10 μ M sorafenib (Sor) for the designated intervals, after which ROS production was monitored as indicated in Materials and Methods. Values represent the means for three separate experiments performed in triplicate and are expressed as increases (*n*-fold) relative to values for nontreated cells. (B) Jurkat cells inducibly expressing constitutively active MEK1 were left untreated (left) or treated with 2 μ g/ml doxycycline (DOX) (right) for 24 h and then exposed to 10 μ M sorafenib for an additional 1 h, after which ROS production was monitored as indicated in Materials and Methods. (C) U937 (left) and Jurkat (right) cells were treated with BAPTA-AM for 30 min before exposure to 10 μ M sorafenib (Sor) for 1 h, after which ROS production was evaluated as described in Materials and Methods. C, control.

chondria (4). Although the precise mechanism underlying this event is incompletely understood, this phenomenon is thought to play an important role in the lethal effects of multiple chemotherapeutic drugs (4). Consequently, the possibility that exposure to sorafenib might increase ROS production was investigated. As shown in Fig. 11A, time course studies revealed that exposure to sorafenib resulted in a rapid and pronounced increase in ROS production in U937 as well as Jurkat cells. However, while pretreatment of U937 cells with the

MnSOD2 mimetic Mn-TBAP in conjunction with PEG-catalase significantly reduced sorafenib-mediated ROS production (see Fig. S6A in the supplemental material), no attenuation of cell death was observed (see Fig. S6B in the supplemental material). Moreover, analogous to previous results, induction of constitutively active MEK1 had no effect on sorafenib-mediated ROS production (Fig. 11B).

To establish the hierarchy between ROS production and calcium mobilization, calcium was depleted by culturing cells in the presence of the calcium chelator BAPTA-AM. Notably, pretreatment with BAPTA-AM (3 μ M) completely inhibited sorafenib-mediated ROS production in U937 as well as Jurkat cells (Fig. 11C), suggesting that calcium mobilization was responsible for ROS production. However, BAPTA-AM and EGTA, neither of which prevents ER calcium store depletion, failed to diminish sorafenib-mediated lethality (see Fig. S6C in the supplemental material). These findings suggest, albeit indirectly, that depletion of ER calcium stores, rather than an increase in cytosolic Ca^{2+} , may contribute to or be responsible for sorafenib-mediated lethality.

DISCUSSION

Sorafenib, originally developed as a specific C-Raf and B-Raf inhibitor, is emerging as a promising targeted agent that may possess significant antitumor activity in certain malignancies (e.g., renal cell carcinoma) (1, 50, 51). In view of the importance of Raf dysregulation in transformation, it was tempting to speculate that sorafenib would kill transformed cells by interrupting the MEK1/2-ERK1/2 pathway. However, the functional role that MEK1/2-ERK1/2 inhibition plays in sorafenib-mediated lethality has not yet been fully characterized. In this context, we recently reported that sorafenib induces a striking increase in apoptosis in human leukemia cells through a mechanism involving Mcl-1 translation inhibition (45). Interestingly, Mcl-1 translation inhibition was independent of MEK/ERK inactivation, leading us to hypothesize that sorafenib may kill cells through a MEK1/2-ERK1/2-independent mechanism. The findings described in this communication demonstrate for the first time that sorafenib induces cell death in human leukemia cells through a mechanism that primarily involves induction of ER stress rather than inactivation of the MEK1/2-ERK1/2 pathway.

Results of the [35 S]methionine incorporation assay revealed that sorafenib diminished general protein translation. One plausible explanation for general protein translation inhibition is induction of the UPR, an adaptive process that blocks protein translation and allows cells to compensate for protein accumulation and misfolding in the ER (61, 63). Notably, treatment with sorafenib resulted in a rapid increase in eIF2 α and PERK phosphorylation, GADD153 and GADD34 accumulation, and XBP1 splicing. These events represent prototypical markers of the ER stress-dependent UPR signaling pathway (53, 63). Given the well-established role of eIF2 α phosphorylation in protein translation inhibition (2, 53), it is tempting to speculate that sorafenib-mediated protein synthesis inhibition is mediated by eIF2 α phosphorylation. However, in view of recent evidence that sorafenib inhibits phosphorylation of the eIF4E translation initiation factor (45), the pos-

sibility that this action also contributes to translation inhibition cannot be excluded.

It is also noteworthy that in contrast to the classical ER stress inducer thapsigargin, which is known to induce the antiapoptotic ER chaperone molecules GRP78 and GRP94 in most cell types, sorafenib did not upregulate these proteins. Instead, sorafenib diminished the expression of GRP78 and blocked thapsigargin-mediated GRP78 accumulation. The observation that the MEK1/2 inhibitor PD184352 exerted similar actions suggests that these effects very likely represent the consequence of Raf-MEK1/2-ERK1/2 inhibition by sorafenib. Together, these data implicate, for the first time, MEK1/2 activation in GRP78 induction following ER stress. Furthermore, the finding that expression of the antiapoptotic GRP78 protein is diminished by sorafenib distinguishes the actions of this compound from those of classical ER stress inducers such as thapsigargin. It is tempting to speculate that disruption of this putative cytoprotective response may be responsible for or contribute to the lethal actions of sorafenib, at least in human leukemia cells. However, it should be noted that enforced activation of MEK1 failed to confer resistance to sorafenib-mediated apoptosis, suggesting that GRP78 inhibition is not critical to sorafenib-mediated lethality. Alternatively, it is possible that sorafenib may disrupt additional pathways required for GRP78 induction, and as a consequence, reestablishment of MEK1/2 activation is insufficient for GRP78 induction. For example, it is possible that p38 activity, which is known to be inhibited by sorafenib (45), may also be required for GRP78 induction (49).

In addition to these factors, accumulation of GADD153 has been shown to enhance apoptosis in response to ER stress in various systems (18, 24). Unexpectedly, results from studies employing siRNA argue against a functional role for GADD153 in sorafenib-mediated lethality. In this regard, results from a recent report suggest a protective role for GADD153 in cell death mediated by fluoride, an agent that induces ER stress in the mouse ameloblast-derived cell line LS8 as well as in MEF cells (29). Finally, induction of constitutively active MEK1 failed to prevent eIF2 α phosphorylation or GADD153 accumulation. Conversely, inhibition of MEK1/2-ERK1/2 activation by the pharmacologic MEK1/2 inhibitor U0126 was unable to increase eIF2 α phosphorylation. Collectively, these observations indicate that the ability of sorafenib to trigger these components of the UPR is largely independent of effects on the Raf-MEK1/2-ERK1/2 cascade.

Results of studies employing siRNA or dominant-negative PERK argue strongly that PERK activation plays a protective role against sorafenib-mediated cell death. Notably, sorafenib-mediated eIF2 α phosphorylation was substantially diminished when PERK activity was specifically abrogated either by siRNA or by a dominant-negative construct, an event associated with a significant increase in sorafenib-mediated lethality. While these findings clearly implicate PERK in eIF2 α phosphorylation following exposure of cells to sorafenib, the other eIF2 α kinases, GCN2, PKR, and HRI (2), did not appear to play a major role in this phenomenon. The present findings are also consistent with the results of previous studies demonstrating a role for PERK in eIF2 α phosphorylation in response to certain ER stress inducers, including thapsigargin and tunicamycin (3, 20, 21), as well as evidence that abrogation of PERK activation renders cells more susceptible to lethal actions of

these agents (20). However, in contrast to its role in protein translation inhibition, the role of eIF2 α phosphorylation in cell death regulation can be pleiotropic and may vary with the nature of stress or cell type. For example, eIF2 α phosphorylation has been shown to protect cells against ER stress inducers such as thapsigargin and tunicamycin (20, 33, 55). In marked contrast, Perkins and Barber (41) reported no effect of eIF2 α phosphorylation on cell death mediated by several proapoptotic agents known to induce ER stress, including etoposide and tumor necrosis factor alpha, among others. Furthermore, following treatment with the proteasome inhibitor MG132, eIF2 α phosphorylation has been shown to enhance apoptosis in MEF cells (24). The present results suggest that an increase in eIF2 α phosphorylation protects cells from sorafenib-mediated apoptosis and are consistent with the notion that PERK activation diminishes sorafenib-mediated lethality through an eIF2 α -dependent process.

In addition to PERK, IRE1 α and ATF6 represent two other ER transmembrane proteins that serve as proximal sensors of ER stress and mediate the UPR. In response to accumulation of unfolded proteins in the ER, IRE1 α undergoes activation and initiates XBP1 mRNA splicing, resulting in the translation of the transcriptionally active form of XBP1 (5, 65). In the present studies, we found that treatment with sorafenib induced a pronounced increase in IRE1 α protein levels and promoted XBP1 mRNA splicing in association with an increase in the transcriptionally active form of the XBP1 protein. In addition, the findings that knockdown of IRE1 α or XBP1 markedly enhanced and overexpression of IRE1 α significantly attenuated sorafenib-mediated lethality indicate that activation of IRE1 α /XBP1 plays a cytoprotective role against sorafenib-mediated apoptosis. In contrast, based on results of shRNA transfection experiments, no major role for involvement of TRAF2 or JNK1/2 in sorafenib-mediated lethality could be documented. These findings are consistent with results of previous studies demonstrating that the pharmacologic JNK inhibitor SP600125 did not prevent Mcl-1 downregulation (45) or lethality (M. Rahmani et al., unpublished data). In this regard, similar findings have been described in studies of Jurkat cells involving cephalostatin 1, a compound that acts through the induction of ER stress (32). Finally, while the present findings strongly suggest a cytoprotective role for PERK and IRE1 α against sorafenib-mediated lethality and predict that disruption of PERK and IRE1 α activity would markedly enhance the antitumor activity of sorafenib, determination of the functional role of ATF6 in these events requires further investigation.

Calcium mobilization represents a well-documented event in the responses of cells to various stimuli and has been implicated in the regulation of diverse cellular process (4). Elevation of cytosolic-calcium levels can occur through several disparate mechanisms. Among these, depletion of ER calcium stores represents a typical response of cells to ER stress inducers (58). Notably, depletion of ER calcium, rather than increases in cytosolic-calcium level per se (66), is believed to play a critical role in apoptosis induction in response to ER stress. In the present study, sorafenib rapidly induced an increase in cytosolic-calcium levels through a MEK1/2-ERK1/2-independent mechanism. This presumably reflected depletion of ER stores, as sorafenib was unable to increase cytosolic-calcium

levels in cells in which ER stores were already depleted by thapsigargin. Although the precise mechanism by which sorafenib initiates calcium mobilization and the functional role that resulting perturbations in calcium homeostasis play in sorafenib-mediated cell death remain unclear, the possibility that ER depletion of Ca²⁺ triggers ER stress, which is known to be a potent cell death signal (66), seems plausible. Furthermore, sorafenib induced a rapid, pronounced, and sustained increase in calcium-dependent ROS production. In this context, previous studies have implicated calcium mobilization in ROS production in diverse systems (4). Moreover, the induction of oxidative injury, manifested by increased generation of ROS, is known to be an effective inducer of apoptosis (16). Consequently, the ability of sorafenib to induce a robust ROS response argues for its involvement in the cell death process. However, pretreatment of cells with the antioxidants MnTBAP and PEG-catalase, while significantly reducing ROS production, had no major effect on cell death. One possible explanation for this finding is that while ROS production was reduced by pretreatment with these antioxidants, it was not eliminated and therefore remained above threshold levels sufficient to induce cell death. An alternative possibility is that sorafenib induces severe ER stress, a lethal process that operates upstream of ROS generation and whose consequences cannot be prevented by antioxidants.

It is important to note that sorafenib induced caspase-2 and caspase-4 processing, an event which plays an important role in cell death mediated by several drugs known to induce ER stress (9, 8, 23, 31, 64). It should be noted that Fribley et al. reported that siRNA-mediated knockdown of caspase-2 failed to protect human head and neck cancer cells from ER stress-induced lethality mediated by the proteasome inhibitor bortezomib (15). However, in agreement with the majority of previous reports linking caspase-2 and -4 activation to ER stress induction, knockdown of caspase-2 or caspase-4 with siRNA or shRNA, respectively, significantly reduced cell death induced by sorafenib. These observations are similar to findings involving the ER stress inducer thapsigargin. Interestingly, knocking down caspase-9 or caspase-3 by shRNA only modestly reduced sorafenib-mediated apoptosis. It should be noted that results of a recent study (40) indicated that the caspase inhibitor z-VAD-fmk failed to afford significant protection to melanoma cell lines against sorafenib-mediated lethality. Similar results have been observed in U937 cells (M. Rahmani et al., unpublished data). The relative lack of susceptibility of caspase-2 and caspase-4 to inhibition by z-VAD-fmk (14), and the observation that knockdown of caspase-9 and caspase-3, which are major substrates of z-VAD-fmk, exerted only modest effects on sorafenib-mediated lethality, may account for the limited ability of this agent to protect cells from sorafenib-induced cell death. Collectively, these data, along with the finding that caspase-9 activation lies downstream of caspase-4, which is believed to represent the apical caspase in ER stress induction in human cells (23), provide further support for the notion that sorafenib acts primarily through an ER stress-dependent mode of cell killing.

In summary, the present findings indicate that at least in human leukemia cells, sorafenib-mediated cell death proceeds through an ER stress-dependent mechanism rather than through inactivation of the MEK1/2-ERK1/2 cascade. In this

regard, another novel class of agents, i.e., proteasome inhibitors, has been found to exert their lethality, at least in part, through induction of ER stress (15, 24, 36). However, while the latter agents presumably trigger this response by blocking protein degradation, the precise mechanism(s) by which sorafenib initiates ER stress is currently unclear. Nevertheless, the present findings represent a potentially important step in understanding the mechanism of lethality of this agent and may also provide a basis for developing other compounds that trigger ER stress as an anticancer strategy. These findings may also permit a more rational integration of sorafenib into combination regimens for the treatment of leukemia and possibly other malignancies.

ACKNOWLEDGMENTS

We thank J. A. Diehl (University of Pennsylvania) for providing us with the PERK Δ C construct, C. Hetz and L. H. Glimcher (Harvard Medical School) for providing us with the HA-IRE1 α construct, and Mark Lynch (Bayer) and John Wright (Cancer Treatment and Evaluation Program, NCI) for critically reading the manuscript and providing us with sorafenib.

This work was supported by awards CA 63753, CA 93738, and CA 100866 from the National Cancer Institute; award 6045-03 from the Leukemia and Lymphoma Society of America; and awards from the Department of Defense and the V Foundation.

REFERENCES

- Ahmad, T., and T. Eisen. 2004. Kinase inhibition with BAY 43-9006 in renal cell carcinoma. *Clin. Cancer Res.* 2004. **10**:6388S-6392S.
- Boyce, M., and J. Yuan. 2006. Cellular response to endoplasmic reticulum stress: a matter of life or death. *Cell Death Differ.* **13**:363-373.
- Brewer, J. W., and J. A. Diehl. 2000. PERK mediates cell-cycle exit during the mammalian unfolded protein response. *Proc. Natl. Acad. Sci. USA* **97**:12625-12630.
- Brookes, P. S., Y. Yoon, J. L. Robotham, M. W. Anders, and S. S. Sheu. 2004. Calcium, ATP, and ROS: a mitochondrial love-hate triangle. *Am. J. Physiol. Cell Physiol.* **287**:C817-C833.
- Calfon, M., H. Zeng, F. Urano, J. H. Till, S. R. Hubbard, H. P. Harding, S. G. Clark, and D. Ron. 2002. IRE1 couples endoplasmic reticulum load to secretory capacity by processing the XBP-1 mRNA. *Nature* **415**:92-96.
- Carlomagno, F., S. Anaganti, T. Guida, G. Salvatore, G. Troncone, S. M. Wilhelm, and M. Santoro. 2006. BAY 43-9006 inhibition of oncogenic RET mutants. *J. Natl. Cancer Inst.* **98**:326-334.
- Chao, D. T., and S. J. Korsmeyer. 1998. BCL-2 family: regulators of cell death. *Annu. Rev. Immunol.* **16**:395-419.
- Cheung, H. H., K. N. Lynn, P. Liston, and R. G. Korneluk. 2006. Involvement of caspase-2 and caspase-9 in endoplasmic reticulum stress-induced apoptosis: a role for the IAPs. *Exp. Cell Res.* **312**:2347-2357.
- Dahmer, M. K. 2005. Caspases-2, -3, and -7 are involved in thapsigargin-induced apoptosis of SH-SY5Y neuroblastoma cells. *J. Neurosci. Res.* **80**:576-583.
- Dai, Y., M. Rahmani, S. J. Corey, P. Dent, and S. Grant. 2004. A Bcr/Abl-independent, Lyn-dependent form of imatinib mesylate (STI-571) resistance is associated with altered expression of Bcl-2. *J. Biol. Chem.* **279**:34227-34239.
- Dai, Y., C. Yu, V. Singh, L. Tang, Z. Wang, R. McNistry, P. Dent, and S. Grant. 2001. Pharmacological inhibitors of the mitogen-activated protein kinase (MAPK) kinase/MAPK cascade interact synergistically with UCN-01 to induce mitochondrial dysfunction and apoptosis in human leukemia cells. *Cancer Res.* **61**:5106-5115.
- Davies, H., G. R. Bignell, C. Cox, P. Stephens, S. Edkins, S. Clegg, J. Teague, H. Woffendin, M. J. Garnett, W. Bottomley, N. Davis, E. Dicks, R. Ewing, Y. Floyd, K. Gray, S. Hall, R. Hawes, J. Hughes, V. Kosmidou, A. Menzies, C. Mould, A. Parker, C. Stevens, S. Watt, S. Hooper, R. Wilson, H. Jayatilake, B. A. Gusterson, C. Cooper, J. Shipley, D. Hargrave, K. Pritchard-Jones, N. Maitland, G. Chenevix-Trench, G. J. Riggins, D. D. Bigner, G. Palmieri, A. Cossu, A. Flanagan, A. Nicholson, J. W. Ho, S. Y. Leung, S. T. Yuen, B. L. Weber, H. F. Seigler, T. L. Darrow, H. Paterson, R. Marais, C. J. Marshall, R. Wooster, M. R. Stratton, and P. A. Futreal. 2002. Mutations of the BRAF gene in human cancer. *Nature* **417**:949-954.
- Derenne, S., B. Monia, N. M. Dean, J. K. Taylor, M. J. Rapp, J. L. Harousseau, R. Bataille, and M. Amiot. 2002. Antisense strategy shows that Mcl-1 rather than Bcl-2 or Bcl-x(L) is an essential survival protein of human myeloma cells. *Blood* **100**:194-199.
- Ekert, P. G., J. Silke, and D. L. Vaux. 1999. Caspase inhibitors. *Cell Death Differ.* **6**:1081-1086.
- Fribley, A., Q. Zeng, and C. Y. Wang. 2004. Proteasome inhibitor PS-341 induces apoptosis through induction of endoplasmic reticulum stress-reactive oxygen species in head and neck squamous cell carcinoma cells. *Mol. Cell. Biol.* **24**:9695-9704.
- Haddad, J. J. 2004. Redox and oxidant-mediated regulation of apoptosis signaling pathways: immuno-pharmac-redox conception of oxidative siege versus cell death commitment. *Int. Immunopharmacol.* **4**:475-493.
- Hamanaka, R. B., B. S. Bennett, S. B. Cullinan, and J. A. Diehl. 2005. PERK and GCN2 contribute to eIF2 α phosphorylation and cell cycle arrest after activation of the unfolded protein response pathway. *Mol. Biol. Cell* **16**:5493-5501.
- Han, X. J., J. K. Chae, M. J. Lee, K. R. You, B. H. Lee, and D. G. Kim. 2005. Involvement of GADD153 and cardiac ankyrin repeat protein in hypoxia-induced apoptosis of H9c2 cells. *J. Biol. Chem.* **280**:23122-23129.
- Harding, H. P., I. Novoa, Y. Zhang, H. Zeng, R. Wek, M. Schapira, and D. Ron. 2000. Regulated translation initiation controls stress-induced gene expression in mammalian cells. *Mol. Cell* **6**:1099-1108.
- Harding, H. P., Y. Zhang, A. Bertolotti, H. Zeng, and D. Ron. 2000. Perk is essential for translational regulation and cell survival during the unfolded protein response. *Mol. Cell* **5**:897-904.
- Harding, H. P., Y. Zhang, and D. Ron. 1999. Protein translation and folding are coupled by an endoplasmic-reticulum-resident kinase. *Nature* **397**:271-274.
- Hetz, C., P. Bernasconi, J. Fisher, A. H. Lee, M. C. Bassik, B. Antonsson, G. S. Brandt, N. N. Iwakoshi, A. Schinzel, L. H. Glimcher, and S. J. Korsmeyer. 2006. Proapoptotic BAX and BAK modulate the unfolded protein response by a direct interaction with IRE1 α . *Science* **312**:572-576.
- Hitomi, J., T. Katayama, Y. Eguchi, T. Kudo, M. Taniguchi, Y. Koyama, T. Manabe, S. Yamagishi, Y. Bando, K. Imaizumi, Y. Tsujimoto, and M. Tohyama. 2004. Involvement of caspase-4 in endoplasmic reticulum stress-induced apoptosis and Abeta-induced cell death. *J. Cell Biol.* **165**:347-356.
- Jiang, H. Y., and R. C. Wek. 2005. Phosphorylation of the alpha-subunit of the eukaryotic initiation factor-2 (eIF2 α) reduces protein synthesis and enhances apoptosis in response to proteasome inhibition. *J. Biol. Chem.* **280**:14189-14202.
- Karasarides, M., A. Chioleches, R. Hayward, D. Niculescu-Duvaz, I. Scallion, F. Friedlos, L. Ogilvie, D. Hedley, J. Martin, C. J. Marshall, C. J. Springer, and R. Marais. 2004. B-RAF is a therapeutic target in melanoma. *Oncogene* **23**:6292-6298.
- Kojima, E., A. Takeuchi, M. Haneda, A. Yagi, T. Hasegawa, K. Yamaki, K. Takeda, S. Akira, K. Shimokata, and K. Isobe. 2003. The function of GADD34 is a recovery from a shutoff of protein synthesis induced by ER stress: elucidation by GADD34-deficient mice. *FASEB J.* **17**:1573-1575.
- Koumenis, C., C. Naczki, M. Koritzinsky, S. Rastani, A. Diehl, N. Sonenberg, A. Koromilas, and B. G. Wouters. 2002. Regulation of protein synthesis by hypoxia via activation of the endoplasmic reticulum kinase PERK and phosphorylation of the translation initiation factor eIF2 α . *Mol. Cell. Biol.* **22**:7405-7416.
- Kozpas, K. M., T. Yang, H. L. Buchan, P. Zhou, and R. W. Craig. 1993. MCL1, a gene expressed in programmed myeloid cell differentiation, has sequence similarity to BCL2. *Proc. Natl. Acad. Sci. USA* **90**:3516-3520.
- Kubota, K., D. H. Lee, M. Tsuchiya, C. S. Young, E. T. Everett, E. A. Martinez-Mier, M. L. Snead, L. Nguyen, F. Urano, and J. D. Bartlett. 2005. Fluoride induces endoplasmic reticulum stress in ameloblasts responsible for dental enamel formation. *J. Biol. Chem.* **280**:23194-23202.
- Kuntzen, C., N. Sonuc, E. N. De Toni, C. Opelz, S. R. Mucha, A. L. Gerbes, and S. T. Eichhorst. 2005. Inhibition of c-Jun-N-terminal-kinase sensitizes tumor cells to CD95-induced apoptosis and induces G2/M cell cycle arrest. *Cancer Res.* **65**:6780-6788.
- Lin, C. F., C. L. Chen, W. T. Chang, M. S. Jan, L. J. Hsu, R. H. Wu, M. J. Tang, W. C. Chang, and Y. S. Lin. 2004. Sequential caspase-2 and caspase-8 activation upstream of mitochondria during ceramide and etoposide-induced apoptosis. *J. Biol. Chem.* **279**:40755-40761.
- Lopez-Anton, N., A. Rudy, N. Barth, M. L. Schmitz, G. R. Pettit, K. Schulze-Osthoff, V. M. Dirsch, and A. M. Vollmar. 2006. The marine product cephalostatin 1 activates an endoplasmic reticulum stress-specific and apoptosis-independent apoptotic signaling pathway. *J. Biol. Chem.* **281**:33078-33086.
- Lu, P. D., C. Jousse, S. J. Marciniak, Y. Zhang, I. Novoa, D. Scheuner, R. J. Kaufman, D. Ron, and H. P. Harding. 2004. Cytoprotection by pre-emptive conditional phosphorylation of translation initiation factor 2. *EMBO J.* **23**:169-179.
- Morris, J. A., A. J. Dorner, C. A. Edwards, L. M. Hendershot, and R. J. Kaufman. 1997. Immunoglobulin binding protein (BiP) function is required to protect cells from endoplasmic reticulum stress but is not required for the secretion of selective proteins. *J. Biol. Chem.* **272**:4327-4334.
- Moulding, D. A., R. V. Giles, D. G. Spiller, M. R. White, D. M. Tidd, and S. W. Edwards. 2000. Apoptosis is rapidly triggered by antisense depletion of MCL-1 in differentiating U937 cells. *Blood* **96**:1756-1763.
- Nawrocki, S. T., J. S. Carew, K. Dunner, Jr., L. H. Boise, P. J. Chiao, P. Huang, J. L. Abbruzzese, and D. J. McConkey. 2005. Bortezomib inhibits

- PKR-like endoplasmic reticulum (ER) kinase and induces apoptosis via ER stress in human pancreatic cancer cells. *Cancer Res.* **65**:11510–11519.
37. Nijhawan, D., M. Fang, E. Traer, Q. Zhong, W. Gao, F. Du, and X. Wang. 2003. Elimination of Mcl-1 is required for the initiation of apoptosis following ultraviolet irradiation. *Genes Dev.* **17**:1475–1486.
 38. Nishitoh, H., A. Matsuzawa, K. Tobiume, K. Saegusa, K. Takeda, K. Inoue, S. Hori, A. Kakizuka, and H. Ichijo. 2002. ASK1 is essential for endoplasmic reticulum stress-induced neuronal cell death triggered by expanded polyglutamine repeats. *Genes Dev.* **16**:1345–1355.
 39. Novoa, I., Y. Zhang, H. Zeng, R. Jungreis, H. P. Harding, and D. Ron. 2003. Stress-induced gene expression requires programmed recovery from translational repression. *EMBO J.* **22**:1180–1187.
 40. Panka, D. J., W. Wang, M. B. Atkins, and J. W. Mier. 2006. The Raf inhibitor BAY 43-9006 (Sorafenib) induces caspase-independent apoptosis in melanoma cells. *Cancer Res.* **66**:1611–1619.
 41. Perkins, D. J., and G. N. Barber. 2004. Defects in translational regulation mediated by the alpha subunit of eukaryotic initiation factor 2 inhibit antiviral activity and facilitate the malignant transformation of human fibroblasts. *Mol. Cell. Biol.* **24**:2025–2040.
 42. Pollock, P. M., U. L. Harper, K. S. Hansen, L. M. Yudit, M. Stark, C. M. Robbins, T. Y. Moses, G. Hostetter, U. Wagner, J. Kakareka, G. Salem, T. Pohida, P. Heenan, P. Duray, O. Kallioniemi, N. K. Hayward, J. M. Trent, and P. S. Meltzer. 2003. High frequency of BRAF mutations in nevi. *Nat. Genet.* **33**:19–20.
 43. Proud, C. G. 2005. The eukaryotic initiation factor 4E-binding proteins and apoptosis. *Cell Death Differ.* **12**:541–546.
 44. Rahmani, M., Y. Dai, and S. Grant. 2002. The histone deacetylase inhibitor sodium butyrate interacts synergistically with phorbol myristate acetate (PMA) to induce mitochondrial damage and apoptosis in human myeloid leukemia cells through a tumor necrosis factor-alpha-mediated process. *Exp. Cell Res.* **277**:31–47.
 45. Rahmani, M., E. M. Davis, C. Bauer, P. Dent, and S. Grant. 2005. Apoptosis induced by the kinase inhibitor BAY 43-9006 in human leukemia cells involves down-regulation of Mcl-1 through inhibition of translation. *J. Biol. Chem.* **280**:35217–35227.
 46. Rahmani, M., E. Reese, Y. Dai, C. Bauer, S. G. Payne, P. Dent, S. Spiegel, and S. Grant. 2005. Coadministration of histone deacetylase inhibitors and perifosine synergistically induces apoptosis in human leukemia cells through Akt and ERK1/2 inactivation and the generation of ceramide and reactive oxygen species. *Cancer Res.* **65**:2422–2432.
 47. Rahmani, M., C. Yu, E. Reese, W. Ahmed, K. Hirsch, P. Dent, and S. Grant. 2003. Inhibition of PI-3 kinase sensitizes human leukemic cells to histone deacetylase inhibitor-mediated apoptosis through p44/42 MAP kinase inactivation and abrogation of p21(CIP1/WAF1) induction rather than AKT inhibition. *Oncogene* **22**:6231–6242.
 48. Rajagopalan, H., A. Bardelli, C. Lengauer, K. W. Kinzler, B. Vogelstein, and V. E. Velculescu. 2002. Tumorigenesis: RAF/RAS oncogenes and mismatch-repair status. *Nature* **418**:934.
 49. Ranganathan, A. C., L. Zhang, A. P. Adam, and J. A. Aguirre-Ghiso. 2006. Functional coupling of p38-induced up-regulation of BiP and activation of RNA-dependent protein kinase-like endoplasmic reticulum kinase to drug resistance of dormant carcinoma cells. *Cancer Res.* **66**:1702–1711.
 50. Ratain, M. J., T. Eisen, W. M. Stadler, K. T. Flaherty, S. B. Kaye, G. L. Rosner, M. Gore, A. A. Desai, A. Patnaik, H. Q. Xiong, E. Rowinsky, J. L. Abbruzzese, C. Xia, R. Simantov, B. Schwartz, and P. J. O'Dwyer. 2006. Phase II placebo-controlled randomized discontinuation trial of sorafenib in patients with metastatic renal cell carcinoma. *J. Clin. Oncol.* **24**:2505–2512.
 51. Reddy, G. K., and R. M. Bukowski. 2006. Sorafenib: recent update on activity as a single agent and in combination with interferon-alpha2 in patients with advanced-stage renal cell carcinoma. *Clin. Genitourin. Cancer* **4**:246–248.
 52. Richter, J. D., and N. Sonenberg. 2005. Regulation of cap-dependent translation by eIF4E inhibitory proteins. *Nature* **433**:477–480.
 53. Ron, D. 2002. Translational control in the endoplasmic reticulum stress response. *J. Clin. Investig.* **110**:1383–1388.
 54. Rutkowski, D. T., and R. J. Kaufman. 2004. A trip to the ER: coping with stress. *Trends Cell Biol.* **14**:20–28.
 55. Scheuner, D., B. Song, E. McEwen, C. Liu, R. Laybutt, P. Gillespie, T. Saunders, S. Bonner-Weir, and R. J. Kaufman. 2001. Translational control is required for the unfolded protein response and in vivo glucose homeostasis. *Mol. Cell* **7**:1165–1176.
 56. Sharma, A., N. R. Trivedi, M. A. Zimmerman, D. A. Tuveson, C. D. Smith, and G. P. Robertson. 2005. Mutant V599EB-Raf regulates growth and vascular development of malignant melanoma tumors. *Cancer Res.* **65**:2412–2421.
 57. Singer, G., R. Oldt III, Y. Cohen, B. G. Wang, D. Sidransky, R. J. Kurman, and I. Shih. 2003. Mutations in BRAF and KRAS characterize the development of low-grade ovarian serous carcinoma. *J. Natl. Cancer Inst.* **95**:484–486.
 58. Treiman, M. 2002. Regulation of the endoplasmic reticulum calcium storage during the unfolded protein response—significance in tissue ischemia? *Trends Cardiovasc. Med.* **12**:57–62.
 59. Wertz, I. E., K. M. O'Rourke, H. Zhou, M. Eby, L. Aravind, S. Seshagiri, P. Wu, C. Wiesmann, R. Baker, D. L. Boone, A. Ma, E. V. Koonin, and V. M. Dixit. 2004. De-ubiquitination and ubiquitin ligase domains of A20 down-regulate NF-kappaB signalling. *Nature* **430**:694–699.
 60. Wilhelm, S. M., C. Carter, L. Tang, D. Wilkie, A. McNabola, H. Rong, C. Chen, X. Zhang, P. Vincent, M. McHugh, Y. Cao, J. Shujath, S. Gawlak, D. Eveleigh, B. Rowley, L. Liu, L. Adnane, M. Lynch, D. Auclair, I. Taylor, R. Gedrich, A. Voznesensky, B. Riedl, L. E. Post, G. Bollag, and P. A. Trail. 2004. BAY 43-9006 exhibits broad spectrum oral antitumor activity and targets the RAF/MEK/ERK pathway and receptor tyrosine kinases involved in tumor progression and angiogenesis. *Cancer Res.* **64**:7099–7109.
 61. Wu, J., and R. J. Kaufman. 2006. From acute ER stress to physiological roles of the unfolded protein response. *Cell Death Differ.* **13**:374–384.
 62. Wu, S., Y. Hu, J. L. Wang, M. Chatterjee, Y. Shi, and R. J. Kaufman. 2002. Ultraviolet light inhibits translation through activation of the unfolded protein response kinase PERK in the lumen of the endoplasmic reticulum. *J. Biol. Chem.* **277**:18077–18083.
 63. Xu, C., B. Bailly-Maitre, and J. C. Reed. 2005. Endoplasmic reticulum stress: cell life and death decisions. *J. Clin. Investig.* **115**:2656–2664.
 64. Yeung, B. H., D. C. Huang, and F. A. Sinicrope. 2006. PS-341 (bortezomib) induces lysosomal cathepsin B release and a caspase-2-dependent mitochondrial permeabilization and apoptosis in human pancreatic cancer cells. *J. Biol. Chem.* **281**:11923–11932.
 65. Yoshida, H., T. Matsui, A. Yamamoto, T. Okada, and K. Mori. 2001. XBP1 mRNA is induced by ATF6 and spliced by IRE1 in response to ER stress to produce a highly active transcription factor. *Cell* **107**:881–891.
 66. Yoshida, I., A. Monji, K. Tashiro, K. Nakamura, R. Inoue, and S. Kanba. 2006. Depletion of intracellular Ca(2+) store itself may be a major factor in thapsigargin-induced ER stress and apoptosis in PC12 cells. *Neurochem. Int.* **48**:696–702.
 67. Yu, C., L. M. Bruzek, X. W. Meng, G. J. Gores, C. A. Carter, S. H. Kaufmann, and A. A. Adjei. 2005. The role of Mcl-1 downregulation in the proapoptotic activity of the multikinase inhibitor BAY 43-9006. *Oncogene* **24**:6861–6869.
 68. Yu, C., M. Rahmani, J. Almenara, E. A. Sausville, P. Dent, and S. Grant. 2004. Induction of apoptosis in human leukemia cells by the tyrosine kinase inhibitor adaphostin proceeds through a RAF-1/MEK/ERK- and AKT-dependent process. *Oncogene* **23**:1364–1376.
 69. Zhou, Y., C. Garcia-Prieto, D. A. Carney, R. H. Xu, H. Pelicano, Y. Kang, W. Yu, C. Lou, S. Kondo, J. Liu, D. M. Harris, Z. Estrov, M. J. Keating, Z. Jin, and P. Huang. 2005. OSW-1: a natural compound with potent anticancer activity and a novel mechanism of action. *J. Natl. Cancer Inst.* **97**:1781–1785.